THE JOURNAL OF BIOLOGICAL CHEMISTRY VOL. 291, NO. 51, pp. 26410–26426, December 16, 2016

Receptor Species-dependent Desensitization Controls KCNQ1/KCNE1 K^+ Channels as Downstream Effectors of G_q Protein-coupled Receptors*[S]

Received for publication, July 6, 2016, and in revised form, November 9, 2016 Published, JBC Papers in Press, November 10, 2016, DOI 10.1074/jbc.M116.746974

Marie-Cécile Kienitz[1], **Dilyana Vladimirova, Christian Müller, Lutz Pott, and Andreas Rinne**

From the Institute of Physiology, Ruhr-University Bochum, Universitätsstrasse 150, D-44780 Bochum, Germany

Edited by Henrik Dohlman

Activation of G_q protein-coupled receptors (G_qPCRs) might induce divergent cellular responses, related to receptor-specific activation of different branches of the G_q signaling pathway. Receptor-specific desensitization provides a mechanism of effector modulation by restricting the spatiotemporal activation of signaling components downstream of G_q. We quantified signaling events downstream of G_qPCR activation with FRET-based biosensors in CHO and HEK 293 cells. KCNQ1/KCNE1 channels (I_{Ks}) were measured as a functional readout of receptor-specific activation. Activation of muscarinic M_1 receptors (M_1-Rs) caused robust and reversible inhibition of I_{Ks}. In contrast, activation of α_{1B}-adrenergic receptors (α_{1B}-ARs) induced transient inhibition of I_{Ks}, which turned into delayed facilitation after agonist withdrawal. As a novel finding, we demonstrate that G_qPCR-specific kinetics of I_{Ks} modulation are determined by receptor-specific desensitization, evident at the level of $G\alpha_q$ activation, phosphatidylinositol 4,5-bisphosphate (PIP_2) depletion, and diacylglycerol production. Sustained I_{Ks} inhibition during M_1-R stimulation is attributed to robust membrane PIP_2 depletion, whereas the rapid desensitization of α_{1B}-AR delimits PIP_2 reduction and augments current activation by protein kinase C (PKC). Overexpression of Ca^{2+}-independent PKCδ did not affect the time course of α_{1B}-AR-induced diacylglycerol formation, excluding a contribution of PKCδ to α_{1B}-AR desensitization. Pharmacological inhibition of Ca^{2+}-dependent PKC isoforms abolished fast α_{1B} receptor desensitization and augmented I_{Ks} reduction, but did not affect I_{Ks} facilitation. These data indicate a contribution of Ca^{2+}-dependent PKCs to α_{1B}-AR desensitization, whereas I_{Ks} facilitation is induced by Ca^{2+}-independent PKC isoforms. In contrast, neither inhibition of Ca^{2+}-dependent/Ca^{2+}-independent isoforms nor overexpression of PKCδ induced M_1 receptor desensitization, excluding a contribution of PKC to M_1-R-induced I_{Ks} modulation.

The canonical signaling pathway of activated $G\alpha_q$ subunits comprises stimulation of PLCβ[2] isoforms, hydrolysis of PIP_2 to release inositol trisphosphate (IP_3) and diacylglycerol (DAG), and subsequent Ca^{2+} release from internal stores and DAG-mediated activation of protein kinase C (PKC) (1). More recent data (reviewed in Ref. 2) indicate that the linear pathway from G_qPCR activation to G_q-induced PLC stimulation is inadequate to explain the broad range of (sometimes divergent) cellular responses. Functional diversity upon stimulation of G_q-coupled receptors might reflect differential coupling to $G\alpha_q$ family members, different G_q efficacies for PLCβ activation, or activation of pathways independently of phosphoinositide hydrolysis. Furthermore, receptor-specific targeting of effector molecules has been shown to depend on the spatial proximity of G_qPCR and effector protein (*e.g.* an ion channel) and on the mobility of signal molecules in the plasma membrane (3).

It is conceivable that G_qPCRs can be distinguished by their efficiency to activate different branches of the $G\alpha_q$ signaling pathway, either IP_3-Ca^{2+} or DAG-PKC, as recently shown for KCNQ2/3 channel modulation by $P2Y_2$-R and M_1-R (4, 5). Stimulation of distinct G_q-coupled receptors induces compartment-specific targeting of G_q effector proteins. As reviewed in Refs. 6–9, compartment-dependent translocation of PKC isoforms to the plasma membrane, the nuclear membrane, or the Golgi complex determines specific intracellular responses by placing PKC isoforms in proximity to their interaction partners. By using genetically encoded FRET-based sensors of organelle-specific PKC activity, recent studies provide evidence that location-specific DAG production enables recruitment of PKC isoforms to different intracellular membranes (10, 11). Spatially restricted activation of components downstream of G_q has been shown to modulate several types of ion channels in a receptor species-dependent fashion, *e.g.* N-type Ca^{2+} channels (12), G protein-activated inward-rectifying K^+ (GIRK) channels (3), and KCNQ1/KCNE1 channels (13).

Apart from spatial organization of signaling components, temporal aspects of receptor activation or G protein-effector interactions determine receptor-specific kinetics of G_qPCR signaling. Diversity of GPCR-induced cellular effects might result

* The authors declare that they have no conflicts of interest with the contents of this article.

[S] This article contains supplemental Figs. S1–S5.

[1] To whom correspondence should be addressed. Tel.: 49-234-3229200; Fax: 49-234-3214449; E-mail: cecile.kienitz@rub.de.

[2] The abbreviations used are: PLC, phospholipase C; α_{1A}-AR, α_{1A}-adrenergic receptor; α_{1B}-AR, α_{1B}-adrenergic receptor; M_1-R, muscarinic M_1 receptor; cPKC, conventional protein kinase C; nPKC, novel protein kinase C; DAG, diacylglycerol; GPCR, G protein-coupled receptor; G_qPCR, G_q protein-coupled receptor; PIP_2, phosphatidylinositol-4,5-bisphosphate; IP_3, inositol trisphosphate; GRK, G protein-coupled receptor kinase; DAGR, DAG reporter; aa, amino acid(s); ACh, acetylcholine; Phe, phenylephrine; BAPTA, 1,2-bis(*o*-aminophenoxy)ethane-*N*,*N*,*N*′,*N*′-tetraacetic acid; stauro, staurosporine; DN, dominant-negative.

from activation of multiple G proteins with varying efficacy and kinetics, inducing either fast cellular responses of limited extent through one type of G protein or a slow, but extended response through another (14). Moreover, as reviewed in Ref. 15, the affinity of activated G protein subunits to their specific effectors and their interaction kinetics determine the equilibrium of active and inactive trimeric G proteins and the dynamics of the G protein cycle.

Receptor-specific desensitization might provide a mechanism of effector modulation by restricting the spatiotemporal activation of downstream G_q signaling components. Receptor desensitization in the continuous presence of an agonist terminates the responsiveness of a cell by limiting second messenger formation. A recent study, investigating the role of PKC activation in regulating TRPC6 channel activity, provides evidence that desensitization of the histamine H1 receptor reduces TRPC6 channel activity by rapid termination of DAG production (16). However, whether receptor species-dependent differences in desensitization determine the time course of channel modulation during stimulation of distinct G_qPCRs has not been elucidated. Rapid termination of second messenger production by receptor desensitization delimits activation of downstream effector proteins. Thus, it is conceivable that receptor desensitization reduces the efficiency to activate certain effector proteins but favors activation of other branches of G_q signaling pathways with either faster activation kinetics or higher second messenger affinity.

In the present study, we quantitatively analyzed signaling events downstream of distinct G_qPCRs by means of FRET-based biosensors in a stable KCNQ1/KCNE1-transfected CHO cell line and in HEK 293 cells. I_{Ks} amplitude during G_qPCR stimulation was measured as a functional readout of receptor species-dependent activation of G_q effectors. Our study demonstrates for the first time significant receptor-dependent differences in the time course of G_q protein activation, DAG production (as a prerequisite of PKC activation), and PIP_2 hydrolysis upon stimulation of either adrenergic α_{1B} or muscarinic M_1 receptors. These fundamental differences are attributed to different time courses of receptor desensitization and, as a consequence, induce different time courses of I_{Ks} modulation. Our data provide evidence that receptor-specific desensitization controls PIP_2 reduction and recruitment of different PKC isoforms, thus resulting in different modes of fine-tuning of I_{Ks} activity.

Results

Receptor Species-dependent Desensitization at the Level of $G\alpha_q$ Activation—Activation of G_qPCRs can be measured and quantified by using a FRET-based biosensor that monitors the G_q protein cycle (17). The expression of the G_q protein biosensor and either the α_{1B}-AR or M_1-R in HEK 293 cells allowed us to compare receptor species-dependent temporal properties of G_q protein activation.

As illustrated by the representative recordings in Fig. 1, *A* and *D*, increasing concentrations of phenylephrine (Phe) or acetylcholine (ACh) (ranging from 0.1 nM to 1 μM) result in an incremental increase of G_q activation as monitored by the stepwise decrease of the FRET ratio. The decrease in the FRET ratio (ΔF) was normalized to ΔF_{max} (the FRET signal obtained during a single application of 1 μM Phe or ACh), yielding concentration-response curves for phenylephrine (α_{1B}-AR)- and acetylcholine (M_1-R)-induced G_q activation (Fig. 1, *B* and *E*). Based on the concentration-response curves (revealing EC_{50} values of 37 nM (Phe, α_{1B}-AR) and 14 nM (ACh, M_1-R)), we applied 1 μM Phe as a saturating agonist concentration for α_{1B}-AR activation and 10 μM ACh for maximal M_1-R-induced G_q activation. During sustained α_{1B}-adrenergic receptor activation by phenylephrine, a gradual increase in the FRET ratio, *i.e.* a decline in G_q activation, was observed (Fig. 1*C*). The amount of desensitization was quantified by the ratio $FRET_{30\ s\ after\ peak}/FRET_{peak}$, indicating a reduction of the FRET ratio of 33 $\pm$ 4.5% ($n = 8$, Phe 1 μM) for the α_{1B}-AR (see also supplemental Fig. S1). In contrast, during stimulation of M_1 receptors ($n = 6$, ACh 10 μM), the FRET ratio remained stable (Fig. 1*F*).

It is conceivable that the receptor-specific differences in G protein activation reflect either different rates of desensitization of α_{1B} and M_1 receptors or less efficient coupling of α_{1B} receptors to $G\alpha_q$ subunits as compared with M_1 receptors. We therefore investigated whether receptor species-dependent differences occurred downstream of G_q activation, using FRET sensors for DAG formation and PIP_2 depletion.

Analysis of Receptor Species-dependent Desensitization by Monitoring the Time Course of DAG Formation—To analyze receptor species-dependent aspects of signaling downstream of the G_q protein, we analyzed the time course of DAG formation in HEK cells expressing either α_{1B}-AR or M_1-R and the fluorescent biosensor DAGR. DAGR reports formation of DAG by an increase in FRET ratio, and the time course of DAG formation can be used to analyze the rate of receptor desensitization during agonist exposure (18). The representative recordings in Fig. 2 show effects of G_qPCR stimulation on DAG production during application of Phe (1 μM) and ACh (10 μM). Stimulation of both receptor species caused a comparable, rapid increase in FRET ratio, reflecting activation of PLC and formation of DAG at the plasma membrane. However, DAG production induced by α_{1B} receptors rapidly decayed during stimulation (Fig. 2*A*), an effect that was not observed for the M_1-R (Fig. 2*B*). The summarized data, expressed as the ratio $FRET_{30\ s\ after\ peak}/FRET_{peak}$ in Fig. 2*C*, indicate a more than 50% reduction of the DAG signal during activation of α_{1B} receptors. In contrast, during stimulation of M_1 receptors, we observed only a 10% reduction in DAG.

Receptor species-dependent differences in the time course of DAG reduction persisted across agonist concentrations. In the presence of nonsaturating agonist concentrations (*e.g.* 50 and 200 nM Phe and ACh), we observed a rapid decline of the DAG signal in α_{1B}-AR-, but not in M_1-R-expressing cells (see supplemental Fig. S2). The different time courses of DAG production in α_{1B}- and M_1-R-expressing HEK cells are likely to reflect receptor species-dependent differences in desensitization. Alternatively, differences in receptor expression levels may affect the time course of desensitization.

If this would be the case, any changes of G_qPCR expression levels, controlled by adjusting the amount of transfected cDNA, might either increase or decrease the rate of desensitization of M_1 or α_{1B} receptors. We therefore transfected HEK 293 cells

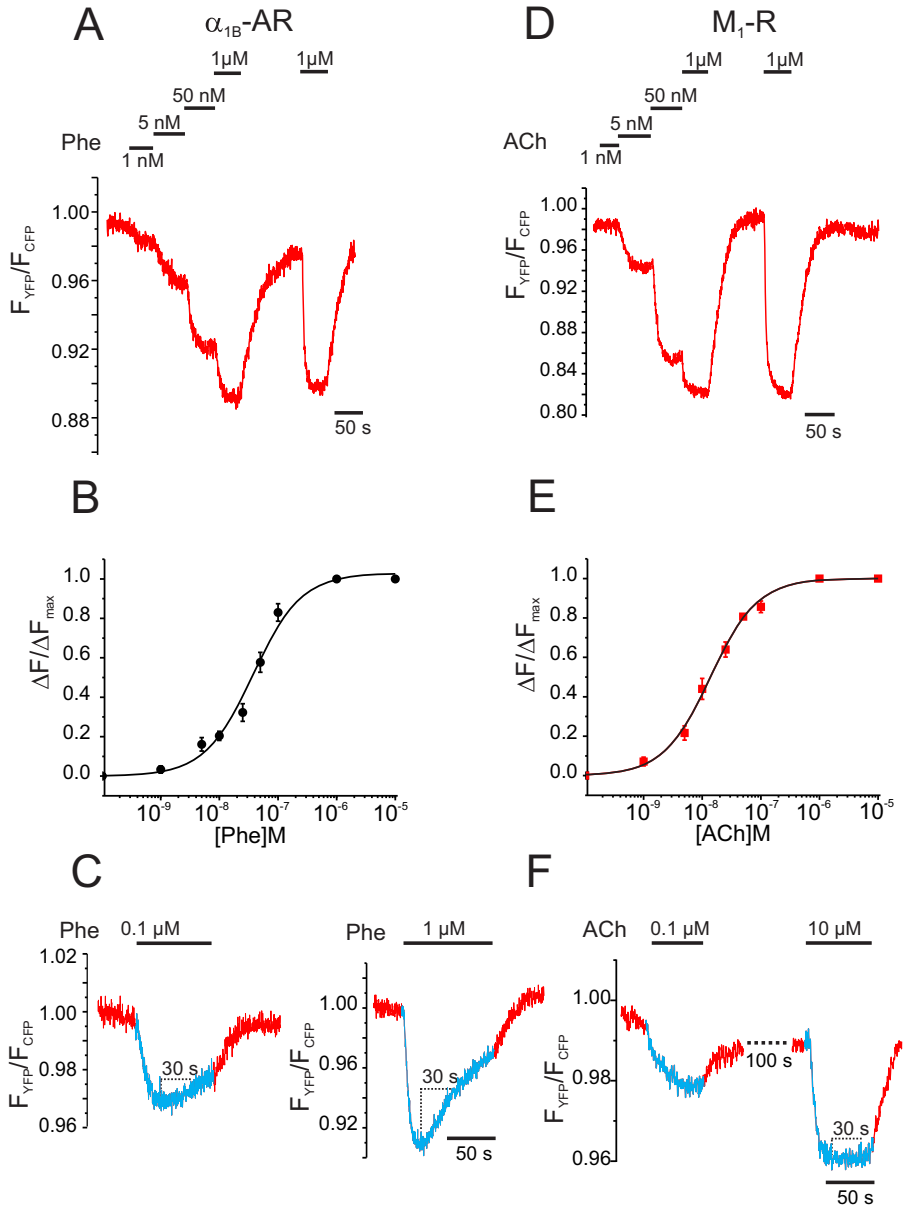

FIGURE 1. **Activation of α_{1B}-AR caused acute desensitization of G protein signaling.** *A*, *C*, *D*, and *F*, representative normalized FRET recordings from α_{1B}-AR- (*A* and *C*) and M_1-R-expressing (*D* and *F*) HEK 293 cells cotransfected with a FRET biosensor measuring G_q activation. Upon activation of G_q by α_{1B} or M_1 receptor stimulation, a decrease in the FRET ratio reflects dissociation of $G\alpha_q$-YFP and $G\beta_1$-Cerulean. *B* and *E*, concentration-response curves for α_{1B}- ($n = 6$) and M_1-R-induced G_q stimulation ($n = 7$). EC_{50} values of α_{1B}- and M_1-induced G_q activation were 37 and 14 nM. Upon application of saturating agonist concentrations (Phe, 1 μM; ACh, 10 μM), fast desensitization was prominent on the level of $G\alpha_q$ activation in α_{1B}-AR- (*C*) but not in M_1-R-expressing cells (*F*). Periods of time plotted in *blue* correspond to times of exposure to agonists. *Error bars* indicate mean ± S.E. of *n* cells; *P*-values less than 0.05 were considered statistically significant.

with different amounts of receptor cDNA and subsequently monitored the time course of DAG formation during receptor stimulation. As shown in Fig. 2, *D–I*, neither increasing the expression level of M_1 receptors nor decreasing the expression of α_{1B} receptors significantly affected the receptor-specific desensitization properties.

Simultaneous Measurements of DAG Production and I_{Ks} Modulation in Stably Transfected KCNQ1/KCNE1 CHO Cells during Stimulation of α_{1B}-AR and M_1-R—Temporal aspects of G_qPCR signaling were further analyzed in CHO cells stably transfected with KCNQ1/KCNE1 and transiently transfected with either α_{1B} or M_1 receptors and the DAG sensor DAGR. We simultaneously measured DAG production and modulation of I_{Ks} amplitude as a functional readout of G_qPCR activation. Previous studies have reported conflicting results on I_{Ks} modulation by different G_q-coupled receptor species.

Both inhibition and activation of KCNQ channels have been reported (13, 19, 20). Some of these receptor species-dependent differences in I_{Ks} modulation might be attributed to activation of different branches of downstream G_q signaling, *e.g.* enhanced PIP_2 depletion or activation of different PKC isoforms.

The representative recordings in Fig. 3 show the relation between G_qPCR desensitization (assessed with the DAGR FRET signal) and I_{Ks} current amplitudes in simultaneous recordings. Application of Phe (1 μM) in α_{1B}-AR-expressing

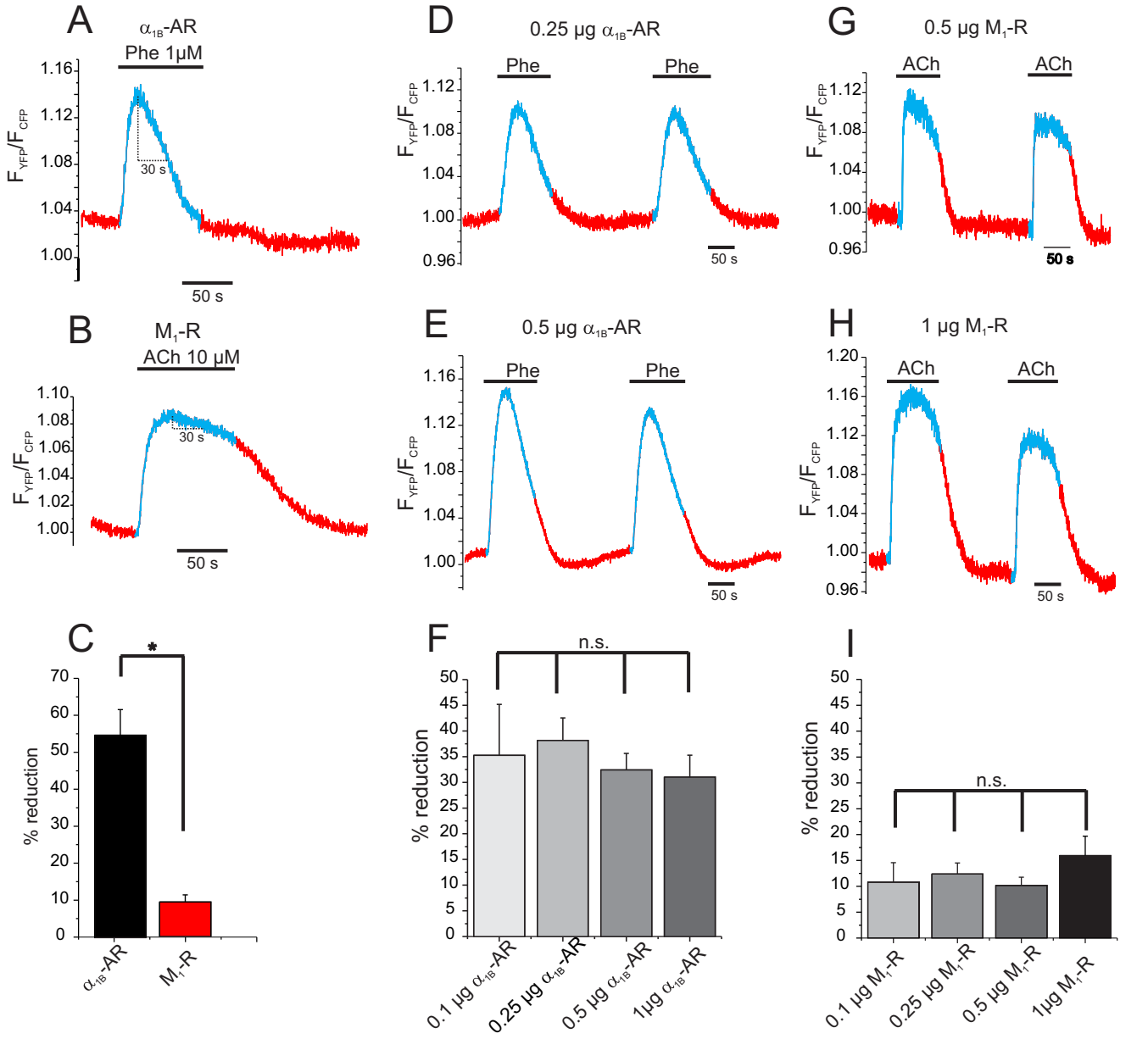

FIGURE 2. **Receptor-specific desensitization at the level of PLC activation and DAG formation is independent of the receptor expression level.** *A* and *B*, representative FRET recordings from α_{1B}-AR- or M_1-R-expressing HEK 293 cells cotransfected with the FRET biosensor DAGR to monitor changes in membrane DAG. Saturating concentrations of agonists were applied as indicated. Periods of time plotted in *blue* correspond to times of exposure to agonists. Note the rapid decay of the FRET ratio in the presence of agonist in α_{1B}-AR- but not in M_1-R-expressing cells. *C*, summarized data of DAG reduction during agonist application (determined by the ratio $FRET_{30\ s\ after\ peak}/FRET_{peak}$), indicating a more than 50% reduction of the DAG signal during activation of α_{1B} receptors ($n = 10$), but only a minor reduction (less than 10%) during stimulation of M_1 receptors ($n = 12$). Significant differences are indicated by *asterisks*. *D* and *E*, representative FRET recordings of HEK 293 cells transfected with 0.25 μg ($n = 7$) or 0.5 μg α_{1B}-AR cDNA ($n = 7$) and DAGR during application of phenylephrine (1 μM). As shown by the summarized data in *F* comparing DAG reduction (measured 30 s after $FRET_{peak}$), decreasing or increasing the expression level of α_{1B} receptors does not affect the rapid desensitization properties (0.1 μg ($n = 4$) or 1 μg of α_{1B}-AR cDNA ($n = 7$)). *G* and *H*, representative FRET recordings of HEK 293 cells transfected with 0.5 μg (*G*, $n = 7$) or 1 μg of M_1-R cDNA (*H*, $n = 7$) and DAGR. Kinetics of DAG formation during application of acetylcholine (10 μM) were not affected by decreasing or increasing the expression level of M_1 receptors (see also summarized data in *I*; 0.1 μg, $n = 6$, 0.25 μg, $n = 5$). *, $p < 0.01$. *n.s.* = not significant. *Error bars* indicate mean ± S.E. of *n* cells.

cells resulted in I_{Ks} inhibition caused by depletion of membrane PIP_2 (13), followed by a sustained increase in current amplitude after agonist withdrawal (Fig. 3, *A* and *C*). This delayed increase in current was lacking after M_1-R stimulation. On the other hand, the initial inhibition of I_{Ks} during agonist application appeared to be more pronounced upon stimulation of M_1 receptors as compared with α_{1B}-adrenergic receptors (Fig. 3, *A* and *C*). The corresponding DAG dynamics in α_{1B}-AR-expressing cells showed a rapid decline during agonist application and had almost returned to basal levels when the α_{1B}-AR-induced I_{Ks} increase occurred (Fig. 3, *B* and *D*). In contrast, stimulation of M_1 receptors induced a more pronounced I_{Ks} inhibition (about 30% of the initial current amplitude in the absence of agonist) as compared with stimulation of α_{1B} receptors (about 15%, Fig. 3*C*). DAG production persisted in the presence of acetylcholine (Fig. 3, *B* and *D*), but failed to stimulate I_{Ks} after

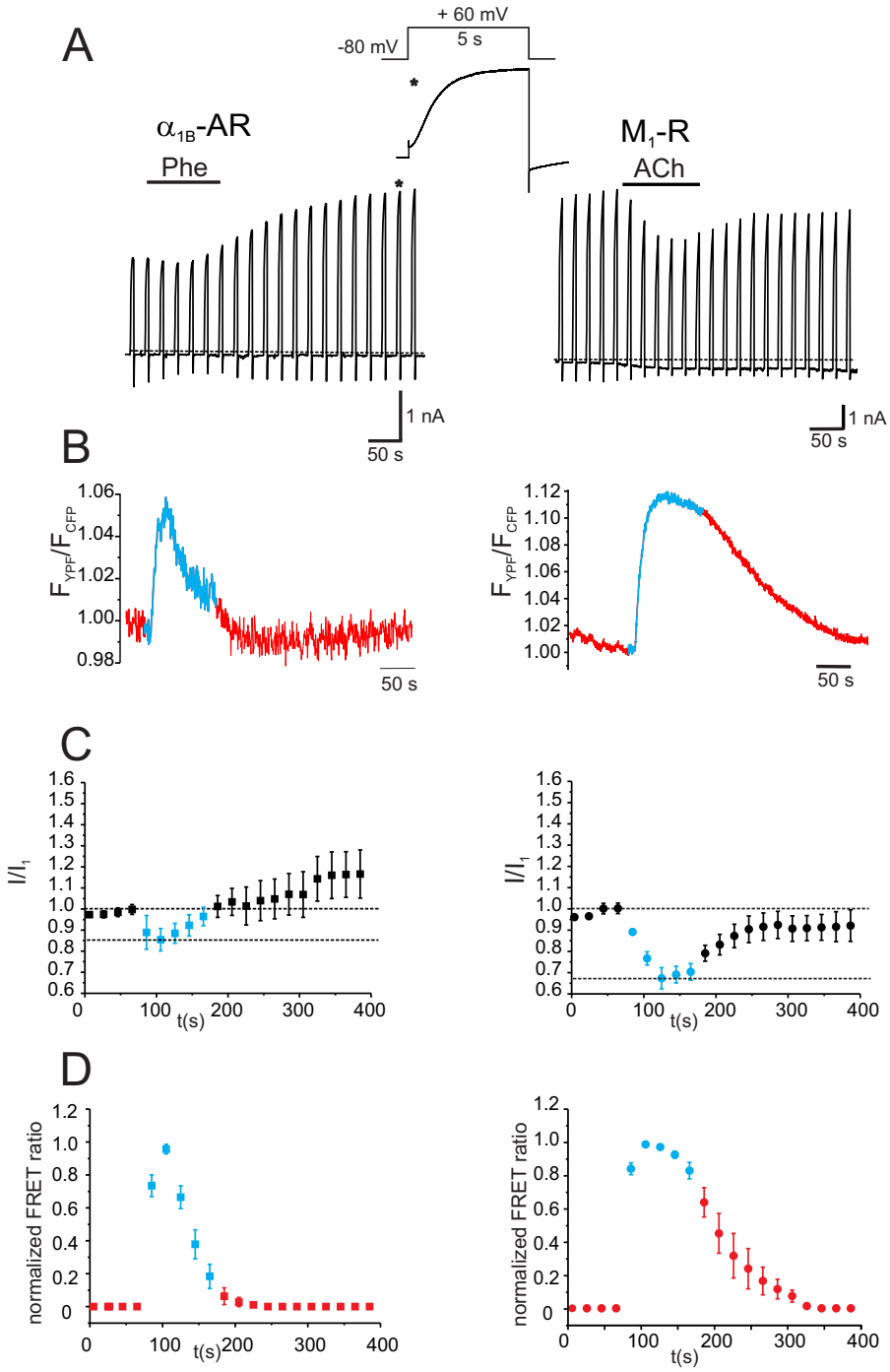

FIGURE 3. **Receptor-specific desensitization determines the time course of I_{Ks} modulation.** *A* and *B*, simultaneous recordings of I_{Ks} (*A*) and DAG production (indicated by an increase in the FRET ratio (*B*)) in stable KCNQ1/KCNE1 CHO cells expressing either α_{1B}-AR or M_1-R and the FRET biosensor DAGR. I_{Ks} was evoked by depolarizing pulses from −80 mV to +60 mV (duration 5 s, 0.05 s^{-1}). An individual I_{Ks} recording (marked by an *asterisk* in *A*) is shown as an *inset*. Application of Phe (1 μM) in α_{1B}-AR-expressing cells resulted in I_{Ks} inhibition and a subsequent increase after agonist withdrawal. Stimulation of M_1 receptors with acetylcholine (10 μM) induced a more pronounced I_{Ks} inhibition, but failed to increase I_{Ks} amplitude. *C*, time course of normalized I_{Ks} (I/I_1) during agonist exposure ($n = 9$ for α_{1B}-AR- and $n = 8$ or M_1-R-expressing cells). The last I_{Ks} current before agonist application was set as I_1. *Dotted lines* indicate the extent of current inhibition. *D*, summarized data of DAG production (normalized FRET ratio), measured simultaneously to I_{Ks}. *Error bars* indicate mean ± S.E. of *n* cells.

agonist withdrawal. (Fig. 3, *A* and *C*). These data suggest that receptor species-dependent differences in G_q effector signaling account for divergent I_{Ks} modulation, supporting the idea that desensitization of different receptor species determines temporal aspects of downstream G_q signaling pathways.

Qualitatively, the temporal aspects of DAG formation during G_qPCR activation are identical in CHO and HEK cells (compare representative traces in Figs. 2 and 3*B*; see also supplemental Fig. S3), indicating that different time courses of DAG production are receptor species-dependent, but independent

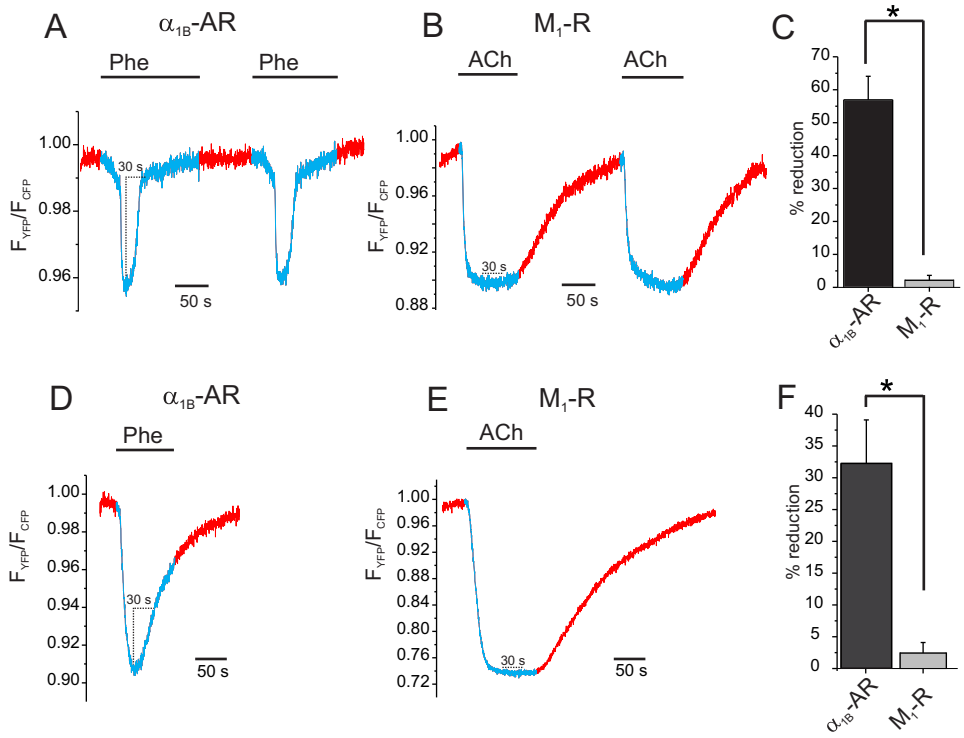

FIGURE 4. **Differences in receptor desensitization between α_{1B}-AR and M_1-R are independent of the cell type.** *A*, *B*, *D*, and *E*, representative FRET recordings from α_{1B}-AR- and M_1-R-transfected CHO (*A* and *B*) and HEK 293 cells (*D* and *E*) cotransfected with a FRET biosensor to monitor changes in membrane PIP_2. Phe (1 μM) and ACh (10 μM) were applied as indicated. Note the rapid decay of the FRET ratio in the presence of agonist in α_{1B}-AR- but not in M_1-R-expressing cells. *C* and *F*, summarized data of PIP_2 reduction during agonist application (determined by the ratio $FRET_{30\ s\ after\ peak}/FRET_{peak}$) (each $n = 11$ for α_{1B}-AR- and M_1-R-expressing CHO cells (*C*) and $n = 9$ and $n = 6$ for α_{1B}-AR- and M_1-R-expressing HEK 293 cells (*F*)). *, $p < 0.01$. *Error bars* indicate mean ± S.E. of *n* cells.

of the cellular background. Moreover, if the receptor-specific time course of the DAG signal reflects intrinsic receptor properties, receptor species-dependent desensitization should be evident at other branches of the G_q signaling pathway, *e.g.* the level of PLC activation and depletion of membrane PIP_2.

Stimulation of α_{1B} Receptors in CHO and HEK Cells Induced a Membrane PIP_2 Depletion That Rapidly Recovered in the Presence of Phenylephrine—We investigated the depletion of membrane PIP_2 following α_{1B} or M_1 receptor stimulation in CHO and HEK cells by utilizing a biosensor that directly reports the depletion of membrane PIP_2 during G_qPCR/PLC activation with a decrease in FRET ratio (21, 22). As illustrated in a representative FRET recording in Fig. 4*A*, stimulation of α_{1B} receptors in CHO cells caused a rapid decrease in FRET ratio, reflecting membrane PIP_2 depletion. This α_{1B}-AR-mediated depletion showed a biphasic time course: during application of phenylephrine (1 μM), FRET slowly decreased for about 20 s, followed by a rapid decay. Remarkably, the FRET ratio rapidly returned to baseline levels, indicating PIP_2 replenishment during sustained receptor stimulation. In contrast, exposure of M_1-R-transfected CHO cells to acetylcholine (10 μM) resulted in a fully reversible decrease in the FRET ratio (Fig. 4*B*) with a rapid onset of PIP_2 depletion that was persistent in the presence of the agonist. Comparing membrane PIP_2 depletion in HEK 293 cells during α_{1B} and M_1 receptor stimulation yielded analogous results, *i.e.* transient reduction and replenishment of PIP_2 in the presence of phenylephrine and persistent PIP_2 depletion during application of acetylcholine (Fig. 4, *D* and *E*). The summarized $FRET_{30\ s\ after\ peak}/FRET_{peak}$ ratios in Fig. 4, *C* and *F*, indicate a reduction of 56% of the PIP_2 signal in CHO cells and a reduction of 32% in HEK 293 cells during activation of α_{1B} receptors and a minor reduction (less than 5%) during stimulation of M_1 receptors in both cell types.

To address whether internalization of the α_{1B} receptor causes its fast desensitization, we analyzed the time courses of arrestin binding as well as of subsequent receptor internalization. Binding of arrestins represents the initial step to prime a GPCR for endocytosis. Of note, the recruitment of arrestins to the receptor prevents G protein binding (23). Thus, recruitment of arrestins could contribute to desensitization of G_q signaling. To estimate the kinetics of arrestin binding for stimulated α_{1B}-ARs and M_1-Rs, we used a FRET assay that monitors the recruitment of Turquoise-labeled β-arrestin to receptors that were labeled with YFP at their C terminus (Fig. 5*A*) (24). The biosensor revealed that recruitment of arrestin occurred fast and with similar kinetics for both receptor subtypes (Fig. 5, *B* and *C*). Therefore, arrestin binding cannot explain the differences in desensitization kinetics of both receptors. Furthermore, the internalization of α_{1B}-AR during long-term exposure to Phe was even slower; in the absence of agonist, we observed a proper membrane localization of α_{1B}-AR-YFP-IL3 (Fig. 5*D*, *panel a*). During exposure to 10 μM Phe, internalization of the receptor was evident by a reduction in plasma membrane fluorescence and formation of intracellular punctae, starting between 15 and 30 min of incubation time (Fig. 5*D*, *panels d–g*).

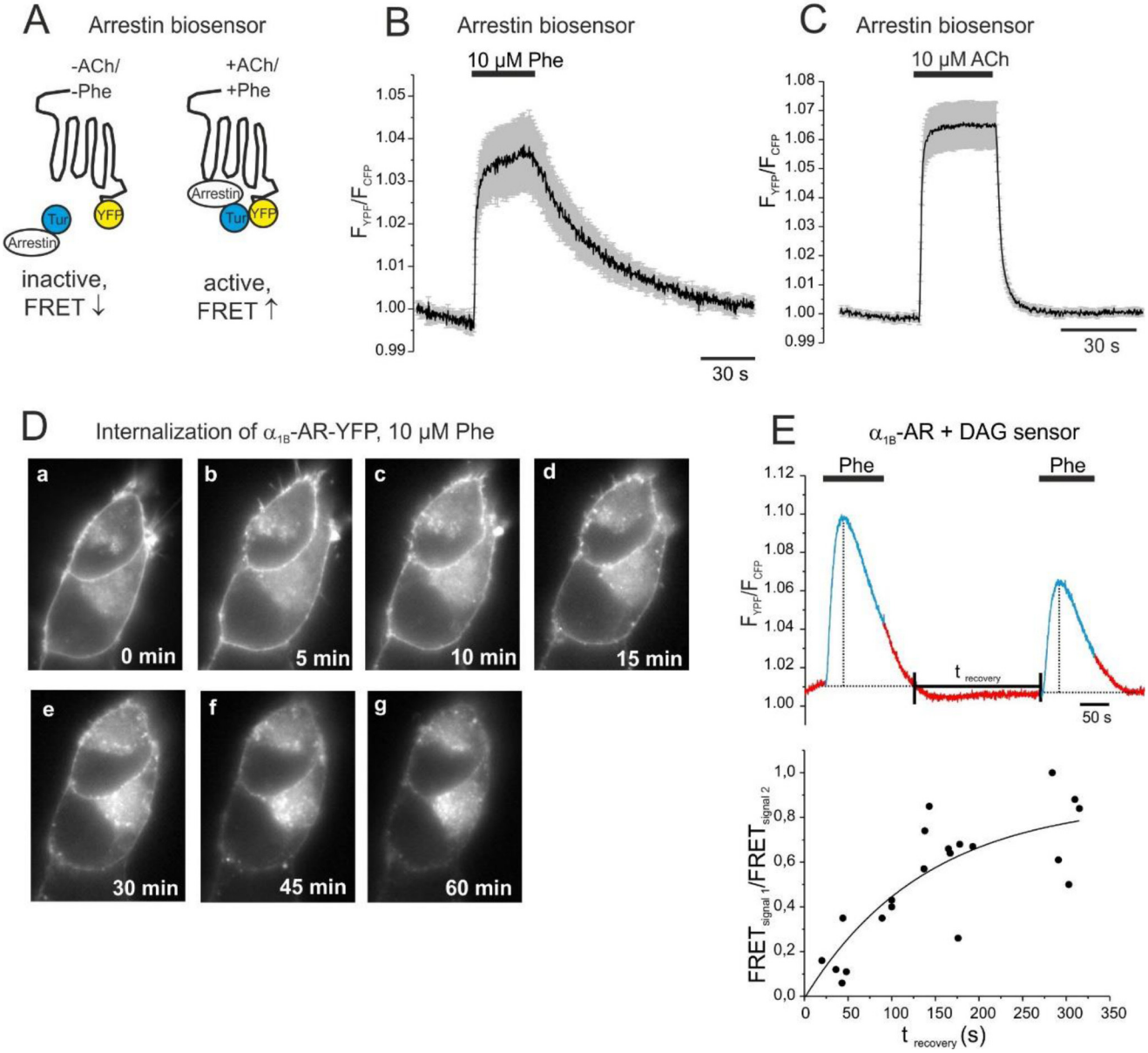

FIGURE 5. **Arrestin binding of α_{1B}-AR-and M_1-R and internalization of α_{1B}-AR-YFP.** *A*, schematic of a FRET assay that detects recruitment of Turquoise (*Tur*)-labeled arrestin3 to the activated α_{1B}-AR-YFP or M_1-R-YFP. *B*, application of 10 μM Phe to HEK 293 cells expressing α_{1B}-AR/arrestin FRET biosensor resulted in rapid increase in the FRET ratio, reflecting receptor activation and recruitment of arrestin3 ($n = 7$). *C*, application of 10 μM ACh to HEK 293 cells expressing the M_1-R/arrestin3 biosensor ($n = 11$) caused a rapid increase in the FRET ratio with similar kinetics of arrestin binding as observed for the α_{1B}-AR. *D*, representative time course of internalization of α_{1B}-AR-YFP-IL3. The time series shows a representative HEK 293 cell expressing α_{1B}-AR-YFP-IL3 before and during long-term exposure to 10 μM Phe. The receptor is localized to the cell membrane before agonist was applied (*panel a*). During incubation with Phe, the membrane staining started to fade away after 15 min (*panel d*), and formation of punctae was visible. The membrane localization was strongly reduced between 45 min (*panel f*) and 60 min (*panel g*) of incubation with agonist. The FRET traces shown in *B* and *C* are presented as mean (*black line*) ± S.E. (*gray shading*). *E*, representative FRET traces from α_{1B}-AR/DAGR-transfected HEK cells. To evaluate recovery from desensitization, DAG signals, evoked by a second application of phenylephrine (1 μM), were normalized to the first DAG signal and plotted against recovery time (defined as the time interval between termination of the first DAG signal and increase of the second signal). Data were fitted with a monoexponential function.

This is in line with the time course for internalization of this receptor in a previous study (25) and is significantly slower (up to 15 min) than the time course of acute desensitization observed in our experiments (*e.g.* see Fig. 2 with complete desensitization of α_{1B} receptors within 60 s of agonist application). These results confirm that neither recruitment of arrestins nor an internalization of the α_{1B}-AR caused its acute desensitization.

We further investigated recovery from α_{1B}-AR desensitization by consecutive applications of phenylephrine (1 μM) with variable time intervals. The second Phe-induced DAG signal was normalized to the first DAG signal and plotted against recovery time (defined as the time interval between termination of the first DAG signal and increase of the second signal). As shown in Fig. 5*E*, up to 80% recovery of the DAG signal was achieved within 300 s. Although we did not determine the molecular mechanism of recovery from desensitization, its rapid time course excludes receptor endocytosis/recycling as the underlying mechanism. Thus, desensiti-

zation and recovery from desensitization are most likely related to direct modifications of the receptor protein, such as phosphorylation/dephosphorylation.

Contribution of PKC Isoforms to Acute α_{1B} Receptor Desensitization—Receptor phosphorylation has been shown to be the earliest biochemical event in homologous and heterologous α_{1B} receptor desensitization either by G protein-coupled receptor kinases (GRK) or by PKC (26). Both *conventional* PKC isoforms (cPKCs, Ca^{2+}- and DAG-dependent) and *novel* PKC isoforms (nPKCs, DAG-dependent, but Ca^{2+}-independent) are downstream effectors of G_q-coupled receptor signaling pathways (27), but their contribution to homologous desensitization of α_{1B}-R is still undefined. We aimed to investigate the contribution of different PKC isoforms to homologous G_qPCR desensitization either by isoform-specific pharmacological PKC inhibition or by manipulating PKC expression levels.

In a first series of experiments, the contribution of PKC to homologous α_{1B} receptor desensitization was analyzed in HEK cells cotransfected with α_{1B}-AR and DAGR by application of the protein kinase inhibitor staurosporine. In the continuous presence of staurosporine (100 nM, 2-h incubation time, with staurosporine in the recording solution), the acute phase of α_{1B} receptor desensitization was completely abrogated (see the representative FRET recordings in Fig. 6, *A* and *B*). As indicated by the summarized data in Fig. 6*G*, comparing the ratio $FRET_{30\ s\ after\ peak}/FRET_{peak}$ in the presence or absence of staurosporine, reduction of the DAG signal during agonist application was markedly diminished by staurosporine.

Staurosporine is a nonspecific protein kinase inhibitor that does not discriminate between PKC isoforms. To evaluate the contribution of different PKC isoforms to homologous desensitization of α_{1B} receptors, we either inhibited cPKCs (Fig. 6, *E* and *F*) or coexpressed the nPKC isoform PKCδ as WT PKCδ (Fig. 6*C*) or as the inactive mutant PKCδ DN (Fig. 6*D*). Activation of α_{1B} receptors in the presence of either WT PKCδ or PKCδ DN resulted in DAG formation that rapidly declined to a similar rate as compared with control conditions (see also Fig. 6*G*), suggesting that PKCδ does not contribute to the acute phase of α_{1B} receptor desensitization.

To reduce activation of cPKCs, we dialyzed α_{1B}-AR/DAGR-cotransfected HEK cells with the Ca^{2+} chelator BAPTA (5 mM) via the patch pipette and measured the time course of DAG decay in the presence of 1 μM Phe. As depicted in Fig. 6, *E* and *G*, buffering the increase in $[Ca^{2+}]_i$ by BAPTA abolished the acute phase of α_{1B} receptor desensitization. The PKC inhibitor Gö6976 inhibits the cPKC isoforms PKCα and PKCβI with an IC_{50} of 2.3 and 6.2 nM without affecting the activity of PKCδ even at high concentrations in the micromolar range (28), thus providing a reliable pharmacological tool to disrupt the activity of cPKCs. In the presence of 10 nM Gö6976 (2-h incubation plus Gö6976 in the recording solution), application of Phe induced DAG formation that did not decline in the presence of agonist, indicating that inhibition of cPKCs eliminated acute desensitization (see also Fig. 6*G*).

Overexpression of WT PKCδ Induced Rapid Desensitization of α_{1A}-AR-induced DAG Formation—The consistent kinetics of α_{1B}-AR-induced DAG signaling upon overexpression of WT PKCδ might exclude a contribution of PKCδ to acute α_{1B} receptor desensitization. To exclude inadequate PKCδ overexpression above the endogenous protein levels, we tested the impact of PKCδ overexpression on the function of the closely related α_{1A}-AR. We investigated DAG kinetics in α_{1A}-AR-expressing HEK cells either under control conditions (Fig. 7*A*) or during coexpression of the WT PKCδ (Fig. 7*B*) or during expression of the catalytically inactive mutant PKCδ DN (Fig. 7*C*). The representative FRET recording in Fig. 7*A* shows a slow decline of the DAG signal during stimulation of α_{1A}-AR with Phe (1 μM). The summarized data in Fig. 7*F*, expressed as the ratio $FRET_{30\ s\ after\ peak}/FRET_{peak}$, indicate a minor reduction of about 12% during activation of α_{1A} receptors under control conditions, but a rapid decline of DAG production upon overexpression of WT PKCδ (Fig. 7*B*, see also Fig. 7*F*). The pronounced reduction of DAG signaling (more than 40%) reflects PKCδ-induced α_{1A}-AR desensitization, which was only observed in the presence of coexpressed PKCδ. To exclude an artifact of protein overexpression, we cotransfected α_{1A}-AR-expressing cells with the PKCδ DN and monitored DAG production. In the presence of the mutant PKCδ DN, DAG kinetics resemble those observed under control conditions (Fig. 7, *C* and *F*), supporting the previous finding that the inactive kinase PKCδ DN specifically inhibits PKCδ-induced signaling pathways (29).

To investigate the contribution of endogenous PKC isoforms to α_{1A}-AR desensitization, we monitored the time course of the α_{1A}-AR-induced DAG signal in the continuous presence of staurosporine (Fig. 7*D*) or Gö6976 (Fig. 7*E*). As shown by the summarized data in Fig. 7*F*, comparing the ratio $FRET_{30\ s\ after\ peak}/FRET_{peak}$, reduction of the DAG signal during agonist application was significantly diminished by staurosporine, but not by Gö6976.

These data indicate a receptor species-dependent and PKC isoform-specific regulation. Inhibition of cPKCs with Gö6976 abrogates desensitization of α_{1B}-ARs, but not of α_{1A}-ARs. Furthermore, although α_{1A}-AR signaling was regulated by PKCδ, there was no direct evidence for a regulation of α_{1B}-AR by PKCδ.

Signaling of M_1-R Was Not Affected by Intracellular Kinases—Agonist-induced desensitization of muscarinic M_1 receptor requires GRK-dependent receptor phosphorylation and recruitment of β-arrestins, resulting in clathrin-dependent receptor internalization (30) (for review, see Ref. 31). Stimulation of PKC has been shown to exert opposing effects on M_1 receptor activity, *e.g.* enhanced acute receptor desensitization (32), a loss of cell surface M_1 receptors, or even no effect on M_1 receptor desensitization or internalization (31). Analogous to the experiments on α_{1B}-R/DAGR-cotransfected cells (Fig. 6), we investigated the contribution of different PKC isoforms to M_1-R signaling by pharmacological inhibition of PKC or coexpression of the wild-type PKCδ. As depicted in Fig. 8, the time course of DAG formation during ACh exposure (10 μM) in the presence or absence of the PKC inhibitors staurosporine and Gö6876 and upon overexpression of PKCδ was indistinguishable, indicating that M_1-R signaling at the level of PLC activation is not modulated by PKC. We did not investigate whether increasing the PKCδ expression level had long-term effects on the number of M_1 receptors at the cell surface. However, during

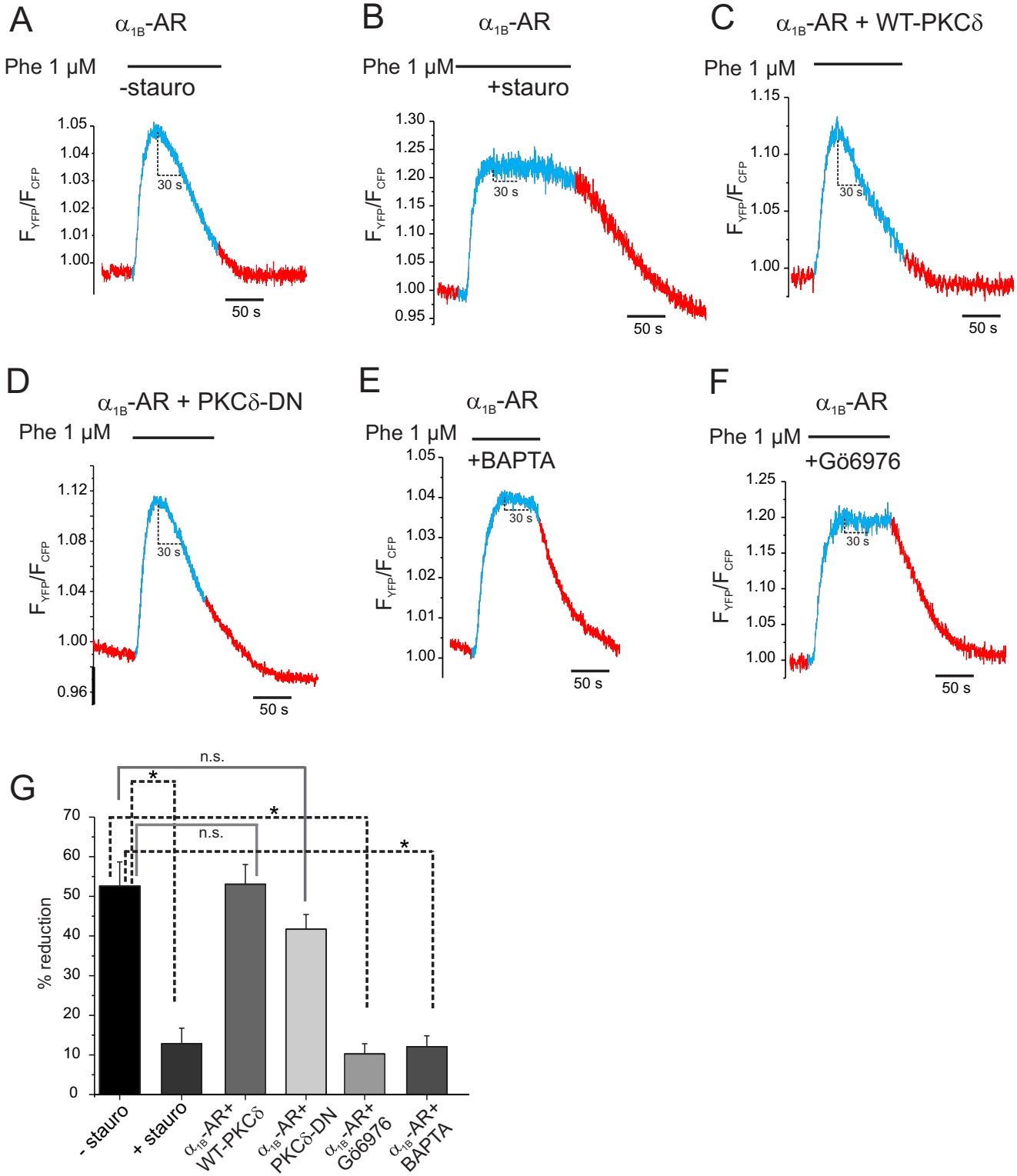

FIGURE 6. **Rapid desensitization of α_{1B}-AR is abolished by inhibition of PKC.** *A* and *B*, FRET recordings from α_{1B}-AR-expressing HEK 293 cells cotransfected with DAGR in the presence (*B*) or absence (*A*) of staurosporine (100 nM, incubation time 2 h, stauro-containing bath solution was used throughout the experiment). *C–F*, rapid desensitization of α_{1B}-AR was abolished by staurosporine, BAPTA (*E*), and Gö6976 (10 nM, incubation time 2 h and throughout the experiment (*F*)), but not by cotransfection with wild-type PKCδ (*C*) or the inactive mutant PKCδ DN (*D*). *G*, summarized data comparing DAG reduction (ratio $FRET_{30\ s\ after\ peak}/FRET_{peak}$) ($n = 12$ for α_{1B}-AR − stauro, $n = 7$ for α_{1B}-AR + stauro, $n = 10$ for α_{1B}-AR + WT PKCδ, $n = 16$ for PKCδ DN, $n = 7$ for BAPTA, and $n = 9$ for α_{1B}-AR + Gö6976). *n.s.* = not significant. *, $p < 0.01$. *Error bars* indicate mean ± S.E. of *n* cells.

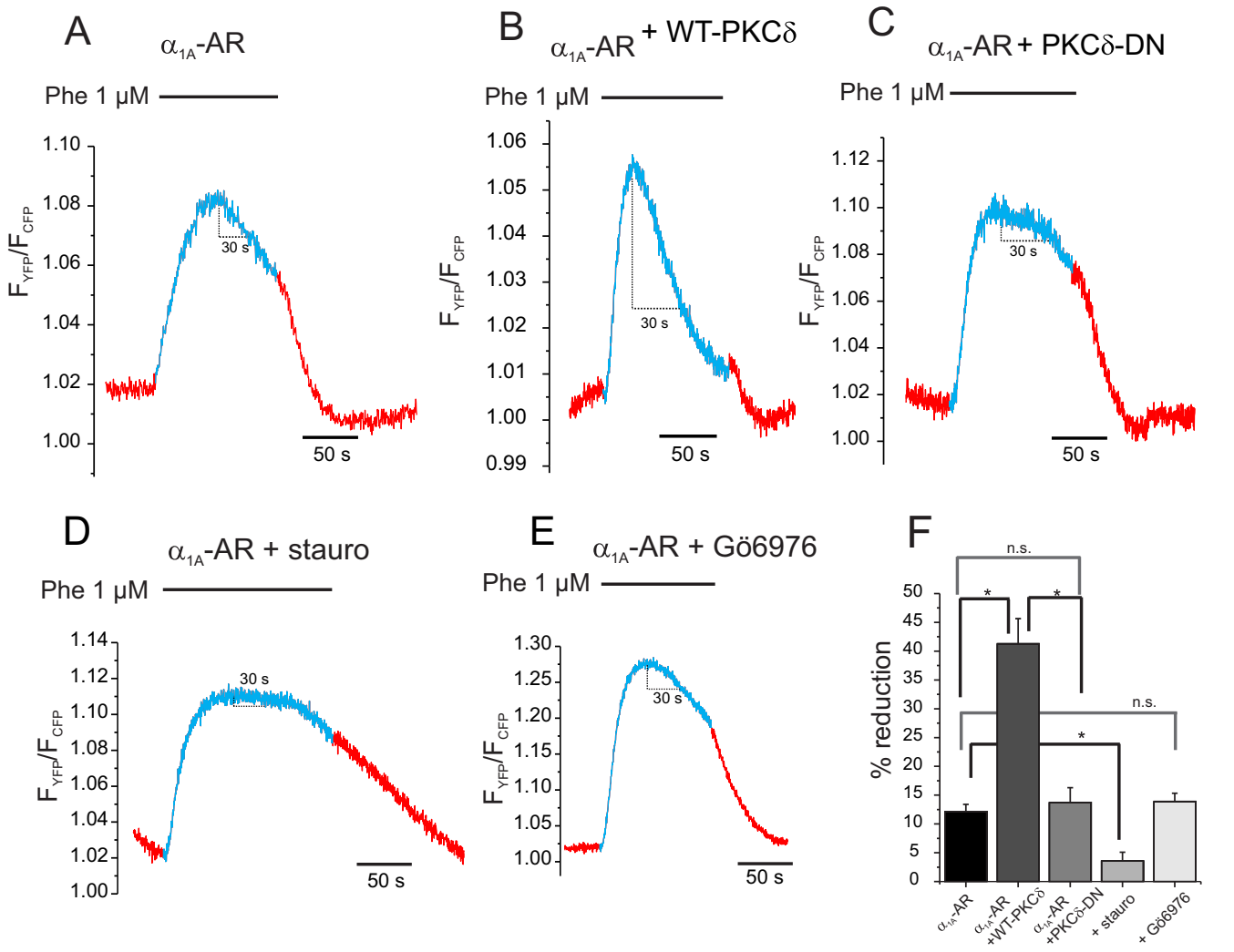

FIGURE 7. **DAG formation in α_{1A}-AR-expressing HEK cells cotransfected with WT PKCδ or the inactive mutant PKCδ DN.** *A–E*, FRET recordings from α_{1A}-AR/DAGR-expressing HEK 293 cells under control conditions (*A*), cotransfected with WT PKCδ (*B*) or the inactive mutant PKCδ DN (*C*), or in the presence of staurosporine (100 nM, *D*) or Gö6976 (10 nM, *E*). Rapid desensitization of α_{1A}-AR was induced by overexpression of WT PKCδ, but not by the inactive mutant PKCδ DN. Incubation of α_{1A}-AR/DAGR-expressing cells with staurosporine (*D*), but not with Gö6976, significantly reduced α_{1A}-AR desensitization. *F*, summarized data comparing DAG reduction (ratio $FRET_{30\ s\ after\ peak}/FRET_{peak}$) for α_{1A}-AR ($n = 17$), α_{1A}-AR + WT PKCδ ($n = 7$), α_{1A}-AR + PKCδ DN ($n = 8$), α_{1A}-AR + stauro ($n = 7$), and α_{1A}-AR + Gö6976 ($n = 10$). *n.s.* = not significant. *, $p < 0.01$. *Error bars* indicate mean ± S.E. of *n* cells.

our experiments (with a duration of 300 – 600 s), receptor internalization is unlikely to occur because we did not observe a PKC-induced reduction in M_1 receptor responsiveness.

Pharmacological PKC Inhibition Reduced the Acute Desensitization of α_{1B}-AR and Modulated I_{Ks} Facilitation—Recent studies on G_qPCR-induced modulation of I_{Ks} suggest fundamental differences in the biophysical channel modulation by Ca^{2+}-dependent and Ca^{2+}-independent PKC isoforms (13, 20), but to date, temporal aspects of cPKC and nPKC activation and their contribution to I_{Ks} modulation are mainly elucidated from kinetic models (13).

Our data suggest that receptor species-dependent differences in desensitization account for a receptor-specific recruitment of different PKC isoforms downstream of PIP_2 depletion and a PKC-induced feedback modulation of receptor activity. Apart from modulating homologous receptor desensitization, the recruitment of different PKC isoforms during G_qPCR activation might shape the temporal signaling properties of downstream G_q signaling effectors.

To address this, we analyzed the modulation of I_{Ks} amplitude in KCNQ1/KCNE1 CHO cells and monitored α_{1B}-AR function simultaneously (DAGR-FRET biosensor) in the presence of PKC inhibitors. As shown previously in Fig. 3*A*, the α_{1B}-AR-induced inhibition of I_{Ks} in the absence of PKC inhibitors was transient and turned into delayed facilitation after agonist withdrawal. Nonspecific inhibition of PKC isoforms with staurosporine reduced the rapid decay of DAG formation in the presence of phenylephrine (Fig. 9, *B* and *D*). Furthermore, PKC inhibition with staurosporine increased α_{1B}-R-induced I_{Ks} reduction and abolished I_{Ks} facilitation (Fig. 9, *A* and *C*).

In the presence of Gö6976, the DAG signal during stimulation of α_{1B} receptors was significantly prolonged (see FRET ratio in Fig. 9*B* and summarized data in 9*D*), indicating a reduction of homologous α_{1B}-AR desensitization. As depicted in Fig. 9*E* (showing the time courses of α_{1B}-AR-induced DAG signals on an expanded time scale), the attenuation of α_{1B}-AR desensitization became evident during sustained agonist application. For example, after 40 s of agonist

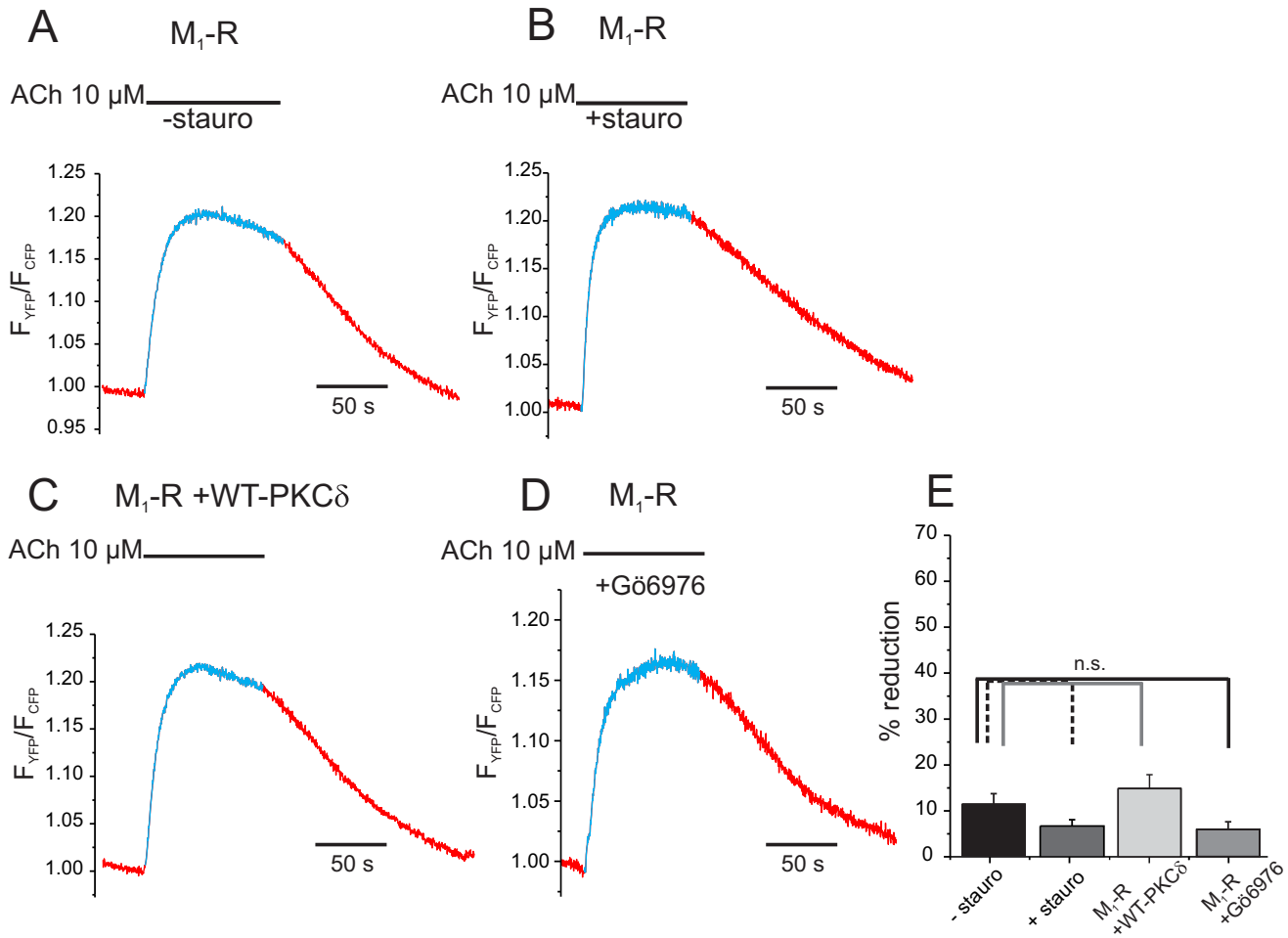

FIGURE 8. **Signaling of M_1-R is not affected by intracellular kinases.** *A–D*, FRET recordings from M_1-R-expressing HEK 293 cells cotransfected with DAGR in the presence (*B*) or absence (*A*) of staurosporine. Neither incubation with staurosporine nor Gö6976 (*D*) nor cotransfection with wild-type PKCδ (*C*) affected the time course of DAG production. *E*, summarized data comparing DAG reduction (measured 30 s after $FRET_{peak}$) ($n = 10$ for M_1-R − stauro, $n = 6$ for M_1-R + stauro, $n = 14$ for M_1-R + WT PKCδ, and $n = 5$ for M_1-R + Gö6976). *n.s.* = not significant. *Error bars* indicate mean ± S.E. of *n* cells.

application (Fig. 9*E* at $t = 145$ s), the Phe-induced DAG signal was decreased to 38% in the absence, but only to 65% in the presence of Gö6976.

Moreover, pharmacological inhibition of Ca^{2+}-dependent PKC isoforms increased the α_{1B}-AR-induced I_{Ks} reduction (Fig. 9*C*), but did not abolish I_{Ks} facilitation after agonist withdrawal. These data indicate a contribution of different PKC isoforms to the time course of α_{1B}-AR-induced I_{Ks} modulation. Activation of Ca^{2+}-dependent PKC isoforms induces rapid α_{1B}-AR desensitization, which delimits PIP_2 depletion, resulting in moderate I_{Ks} inhibition. Disruption of cPKC activation prolongs α_{1B}-AR-induced PIP_2 depletion, thus augmenting I_{Ks} inhibition (compare the extent of current inhibition indicated by *dotted lines* in Figs. 3*C*, *left panel*, and 9*C*). However, a contribution of cPKCs to the current increase after agonist withdrawal can be excluded, because I_{Ks} facilitation was still observed during pharmacological inhibition of cPKCs. In contrast, inhibition of cPKCs and nPKCs by staurosporine abolished I_{Ks} facilitation, suggesting that activation of Ca^{2+}-independent PKC isoforms mediates I_{Ks} increase.

The Rapid Decline of DAG Formation Is Reduced in HEK Cells Expressing the α_{1B}/α_{1A}-CT chimera as Compared with α_{1B}-AR-induced DAG Signals—Phosphorylation sites at the C terminus of α_{1B}-AR have been shown to be critically involved in receptor desensitization (33–35) and receptor endocytosis (36). These phosphorylation sites are not conserved among the other α-adrenergic receptor subtypes. As shown previously, α_{1A}-ARs are less sensitive to agonist-induced desensitization and are phosphorylated to a lesser extent as compared with α_{1B}-AR (34). Because former studies were not designed to analyze dynamic temporal aspects of desensitization, we coexpressed chimeric α_{1B}-AR carrying the C terminus of α_{1A}-AR (α_{1B}/α_{1A}-CT chimera) together with DAGR in HEK 293 cells and compared the agonist-induced DAG dynamics among wild-type α_{1B}-AR, α_{1A}-AR, and the α_{1B}/α_{1A}-CT chimera (Fig. 10). The representative FRET recordings in Fig. 10 show the effects of G_qPCR stimulation on DAG dynamics during application of Phe (1 μM). DAG production in HEK 293 cells rapidly decayed during stimulation of α_{1B} receptors (Fig. 10*A*), but was significantly prolonged in α_{1A}-AR- and α_{1B}/α_{1A}-CT chimera-expressing cells (Fig. 10, *B* and *C*). The summarized data, expressed as the ratio $FRET_{30\ s\ after\ peak}/FRET_{peak}$ in Fig. 10*E*, indicate a more than 50% reduction of the DAG signal during activation of α_{1B} receptors in line with the data shown in Fig. 2, and a significantly smaller reduction during stimulation of α_{1A} receptors (about 15%, the same data as depicted in Fig. 7*D*) and α_{1B}/α_{1A}-CT chimera receptors (about 27%).

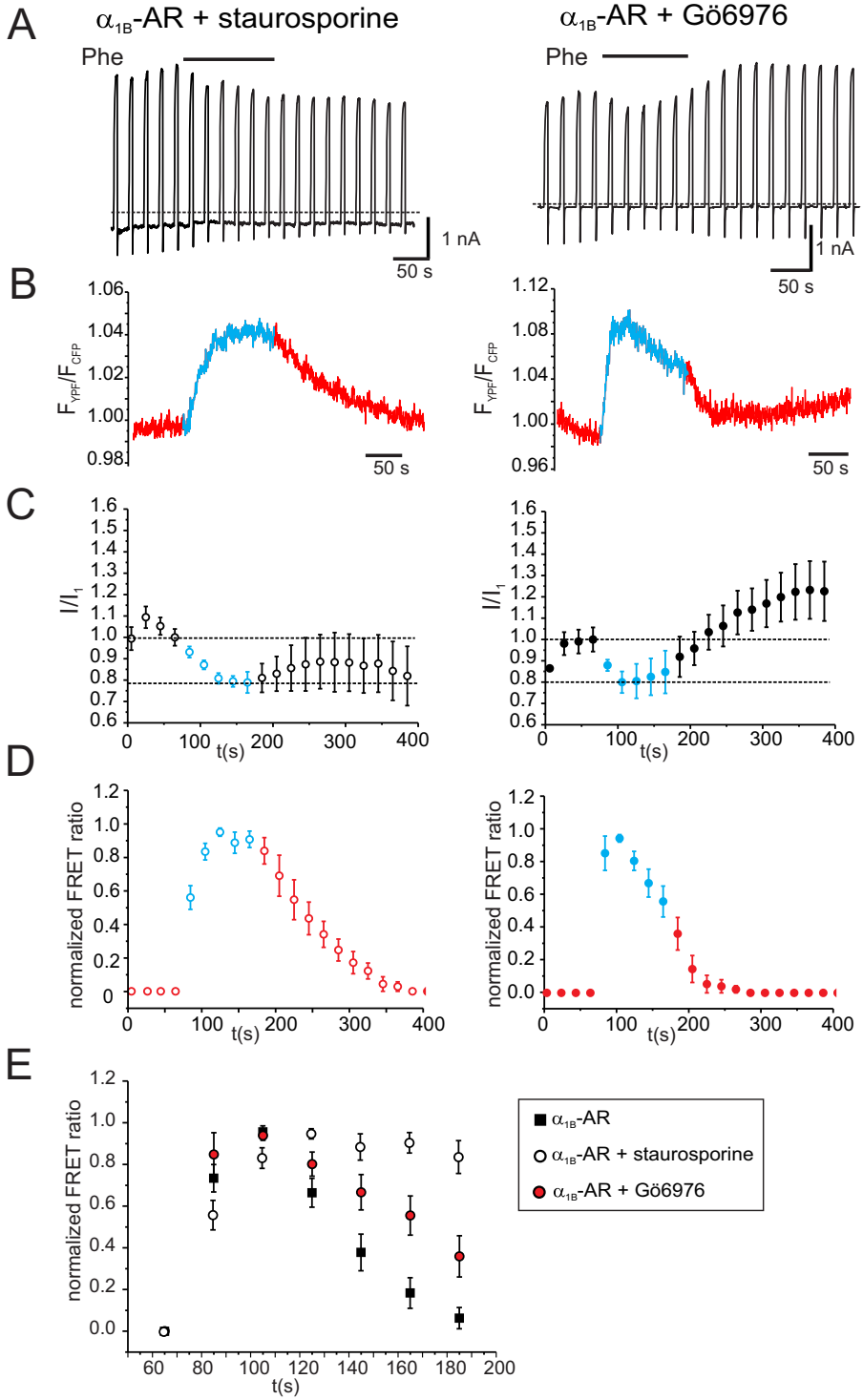

FIGURE 9. **Pharmacological PKC inhibition reduces the acute desensitization of α_{1B}-AR and modulates I_{Ks} facilitation.** *A* and *B*, simultaneous recordings of I_{Ks} (*A*) and DAG production (*B*) in α_{1B}-AR/DAGR-expressing CHO cells (stably transfected with KCNQ1/KCNE1) in the presence of staurosporine (100 nM, 2-h incubation and throughout the experiment, *left panel*) or Gö6976 (10 nM, 2-h incubation and throughout the experiment, *right panel*). Note that both PKC inhibitors significantly reduced the rapid desensitization of α_{1B}-AR, but that I_{Ks} facilitation was maintained in the presence of Gö6976. *C*, time course of normalized I_{Ks} (I/I_1) during phenylephrine (1 μM) exposure. *D*, summarized data of DAG production (normalized FRET ratio), $n = 6$ for α_{1B}-AR + stauro, $n = 6$ for α_{1B}-AR + Gö6976. *E*, DAG signals from *D* displayed on an expanded time scale (for α_{1B}-AR under control conditions, the same data as in Fig. 3*D* are shown on an expanded time scale). *Error bars* indicate mean ± S.E. of *n* cells.

During sustained agonist application (>60 s), the DAG signal declined almost to baseline in α_{1B}-AR-expressing cells, but decayed with a slower time course during stimulation of α_{1A}-AR- and α_{1B}/α_{1A}-CT chimera-AR. As indicated by the summarized data in Fig. 10*F*, comparing the ratio $FRET_{60\ s\ after\ peak}/FRET_{peak}$, the desensitization characteristics of α_{1B}/α_{1A}-CT chimera-expressing cells resemble those observed in wild-type α_{1A}-AR-expressing cells, although desensitization of $\alpha_{1B}/$

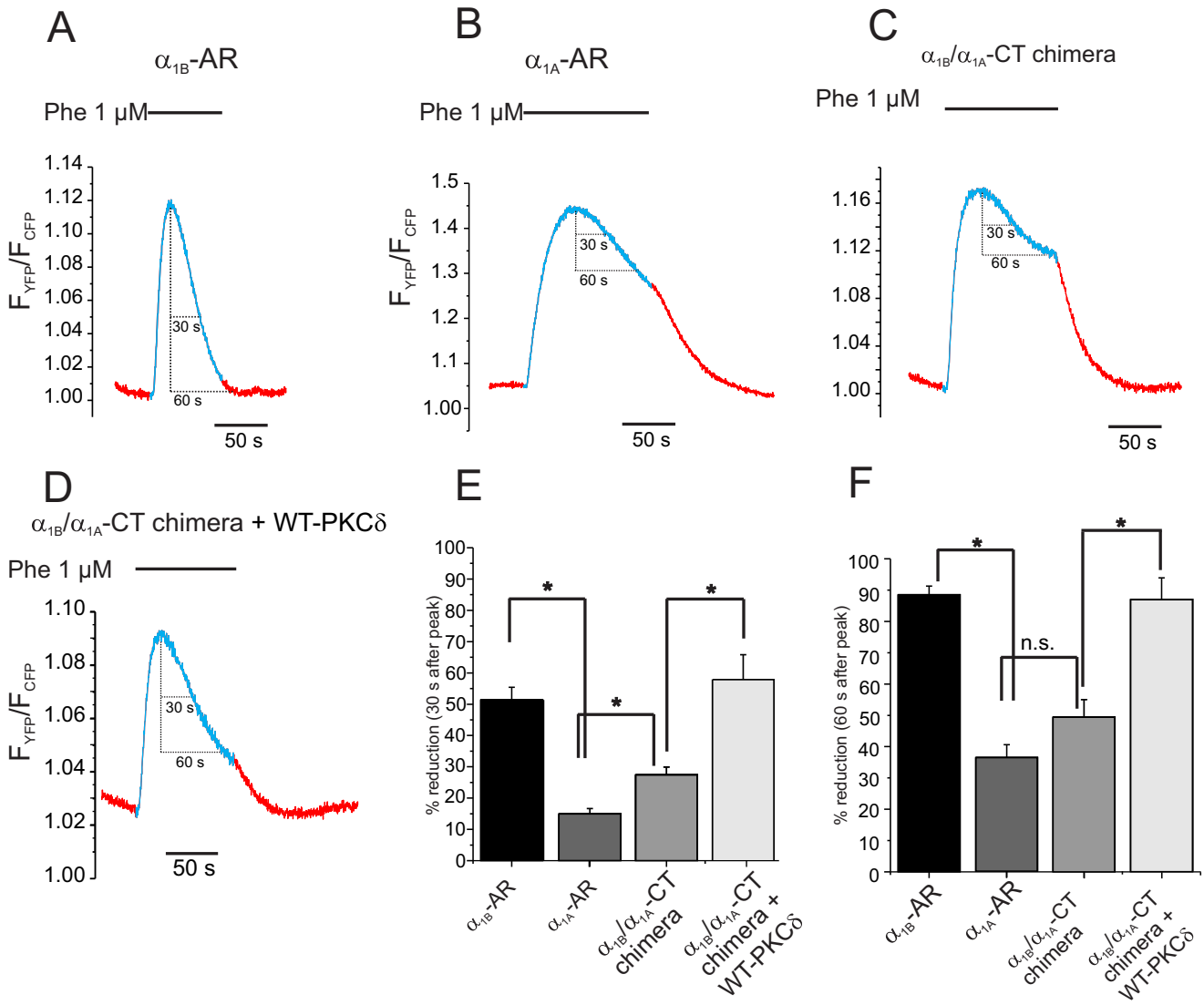

FIGURE 10. **Rapid decline of DAG formation is reduced in HEK cells expressing the α_{1B}/α_{1A}-CT chimera as compared with α_{1B}-AR-induced DAG signals.** *A–D*, FRET recordings of DAG production in α_{1B}-AR-expressing HEK 293 cells (*A*) cotransfected with DAGR or α_{1A}-AR/DAGR- (*B*) or α_{1B}/α_{1A}-CT chimera/DAGR- (*C*) or α_{1B}/α_{1A}-CT chimera/DAGR/WT PKCδ-expressing cells (*D*). Phenylephrine (1 μM) was applied as indicated. Periods of time plotted in *blue* correspond to times of exposure to agonist. Note the rapid decay of the FRET ratio in the presence of agonist in α_{1B}-AR- but not in α_{1A}-AR or α_{1B}/α_{1A}-CT chimera-expressing cells. *E* and *F*, summarized data of DAG reduction during agonist application (determined by the ratio $FRET_{30\ s\ after\ peak}/FRET_{peak}$ (*E*) or $FRET_{60\ s\ after\ peak}/FRET_{peak}$ (*F*)), indicating a more than 50% reduction of the DAG signal (within 30 s) during activation of α_{1B} receptors ($n = 14$), a minor reduction (about 15%) during stimulation of α_{1A} receptors ($n = 7$), a reduction of about 27% during stimulation of the α_{1B}/α_{1A}-CT chimera ($n = 11$), and a reduction of 58% in α_{1B}/α_{1A}-CT chimera/DAGR/WT PKCδ-expressing cells ($n = 6$). After 60 s of agonist application, the DAG signal decreased by about 90% in α_{1B}-AR-expressing HEK 293 cells, by 34% in α_{1A}-AR-expressing cells, by 50% in α_{1B}/α_{1A}-CT chimera/DAGR-expressing cells, and by 89% in α_{1B}/α_{1A}-CT chimera/DAGR/WT PKCδ-expressing cells. *n.s.* = not significant. *, $p < 0.01$. *Error bars* indicate mean ± S.E. of *n* cells.

α_{1A}-CT chimera-AR occurred slightly faster than those of wild-type α_{1A}-AR (Fig. 10*F*). Furthermore, as for the wild-type α_{1A}-AR, overexpression of WT PKCδ induced pronounced desensitization of α_{1B}/α_{1A}-CT chimera receptors as indicated by the rapid decline of the DAG signal (Fig. 10*D*).

Because the time course of desensitization induced by the chimera is an intermediate between the α_{1B}-AR and α_{1A}-AR desensitization phenotypes, it is proposed that additional regions, apart from the C terminus, contribute to α_{1B} receptor desensitization. Although the identification of additional mechanisms of α_{1B}-AR desensitization is beyond the scope of the present study, the significant reduction of desensitization in chimeric α_{1B} receptors carrying the α_{1A}-AR C terminus emphasizes that the number of phosphorylation sites (*i.e.* the degree of receptor phosphorylation) is directly related to the extent of acute desensitization of the receptors.

Discussion

Spatial and temporal organization of signaling components downstream of $G\alpha_q$ activation is related to distinct cellular responses upon activation of different G_qPCRs (2). Receptor-specific cellular events might be induced by promiscuous coupling of GPCRs to $G\alpha_q$ family members, interaction of $G\alpha_q$ with GRK2 or regulators of G protein Signaling (RGS) proteins, or different affinities of $G\alpha_q$ effector activation (2). Furthermore, functional diversity upon stimulation of G_qPCRs can be determined by spatial proximity of G_qPCRs and signal molecules (3),

by activating different branches of the signaling pathway downstream of $G\alpha_q$ (4, 5), or by connecting signaling enzymes to their substrates in specific microdomains (8).

The aspect of receptor species-dependent desensitization that determines temporal aspects of downstream G protein signaling has not been elucidated so far. In our study, we investigated the receptor-specific desensitization of α_{1B} and M_1 receptors as paradigmatic $G\alpha_q$-coupled receptors (37, 38).

We provide evidence that receptor-specific desensitization shapes the kinetics of G_q signaling, resulting in receptor species-dependent modulation of effectors. By using a variety of FRET-based biosensors, we demonstrated receptor species-dependent differences in desensitization on all levels of downstream G_qPCR signaling, including G protein activation (Fig. 1), PIP_2 depletion upon activation of PLC (Fig. 4), and DAG formation (Fig. 2).

Several lines of evidence support the idea that receptor-specific desensitization reflects intrinsic receptor properties rather than being related to insufficient receptor-G protein coupling or insufficient effector activation. First, receptor-specific desensitization of α_{1B} and M_1 receptors was not abolished upon decreasing or increasing their respective expression levels (Fig. 2) and was present at saturating and moderate agonist concentrations at a given receptor expression level (compare 100 nM *versus* 1 μM responses in Fig. 1). Second, as yielded by the concentration-response curves for α_{1B}-AR- and M_1-R-induced G_q activation (Fig. 1), the agonist concentrations used in the present study induced full activation of G proteins and downstream $G\alpha_q$ components. Third, similar temporal aspects of α_{1B} and M_1 receptor signaling were evident in CHO cells stably expressing KCNQ1/KCNE1 and HEK 293 cells, excluding cell line-dependent differences in rate and extent of receptor desensitization (Fig. 4).

Transient α_{1B}-R activity induces a rapid decline of signaling events downstream of α_{1B} receptor activation, *e.g.* on the level of DAG production. The biosensor DAGR has been validated to report the kinetics of G_qPCR regulation by dynamic DAG formation (39), which correlates with the time course of receptor desensitization. Furthermore, it has been demonstrated that manipulations that impair receptor desensitization (*e.g.* altering receptor expression levels, phosphorylating GPCRs, or silencing GRK2 by siRNA) lead to sustained DAG formation (39).

GPCR desensitization involves biochemical processes with different time frames, including receptor phosphorylation by G protein-coupled receptor kinases or protein kinase C as the earliest biochemical event, receptor internalization, and with a longer time course, changes in the receptor expression level (26). By using site-directed mutagenesis, desensitization-associated serine residues, which are targeted either by GRK2 or by PKC, have been identified in the C terminus of the α_{1B} receptor (35). Although truncation studies demonstrated that homologous desensitization of the α_{1B}-AR depends unequivocally on PKC-induced phosphorylation of serine residues in the C terminus (35, 40), conflicting results were reported upon the contribution of GRK to α_{1B}-AR phosphorylation and desensitization (41, 42), depending on the cell expression system. Mutational studies on hamster α_{1B}-AR indicate that PKC activation and phosphorylation of residues within the C-tail promote rapid receptor internalization (43). More recent studies propose that interactions of α_{1B}-AR with β-arrestin and the clathrin adaptor complex AP2 (36) or with Rab4 and Rab5 proteins that are associated with early endosomes (25) regulate receptor internalization. All receptor modifications stated above may result in termination of receptor signaling by internalization of the receptors.

PKC phosphorylation sites are not conserved among the other α-adrenergic receptor subtypes, and differences in receptor desensitization and internalization between α_{1B}-AR and α_{1A}-AR (with modest internalization of α_{1A}-AR as compared with α_{1B}-AR) are mainly related to receptor subtype-dependent differences in β-arrestin binding (36). A recent study (44) describes that differences in the α-AR subtype internalization account for activation of different, subtype-specific downstream G_qPCR effectors. As revealed by our data (Fig. 5), receptor internalization (with a time course of $\geq$15 min) does not contribute to the acute phase of α_{1B}-AR desensitization (see also Fig. 2), which was almost complete within 60 s of agonist application. In addition, we were able to elicit DAG signals upon repetitive agonist application (Fig. 2), excluding a significant reduction in the number of receptor molecules on the cell surface. Furthermore, the fast recovery from desensitization (Fig. 5) suggests that direct modification of the receptor protein instead of receptor endocytosis is the underlying mechanism of receptor desensitization.

It was not the aim of the present study to investigate α_{1A}-AR desensitization, but previous studies showed significant differences in the extent of phosphorylation between α_{1A}-AR and α_{1B}-AR (34). α_{1A}-ARs are phosphorylated to a lesser extent as compared with α_{1B}-ARs and display only minor desensitization. These data are in line with our observation that overexpression of the wild-type PKCδ, but not of the inactive mutant PKCδ DN, rapidly terminated DAG signaling during α_{1A}-AR stimulation (Fig. 7). Furthermore, these experiments demonstrate the efficiency of PKCδ overexpression. Apparently, overexpression of the wild-type PKCδ augments α_{1A}-AR desensitization. However, the contribution of different PKC isoforms to endogenous α_{1A}-AR signaling is evident from our experiments shown in Figs. 6 and 7. Although staurosporine abrogates desensitization of both α_{1A} and α_{1B} receptors, a contribution of cPKCs to α_{1A}-AR desensitization can be excluded. Inhibition of cPKCs with Gö6976 abolishes acute desensitization of α_{1B} but not of α_{1A} receptors (Figs. 6 and 7), indicating receptor-specific regulation by different PKC isoforms.

Moreover, our experiments investigating the kinetics of α_{1B}/α_{1A}-CT chimera-induced desensitization indicate that the origin of the α-AR subtype C terminus determines the time course and kinetics of receptor desensitization. These data are in line with a previous study (34) on chimeric α_{1A} and α_{1B} receptors, carrying the mutual C-terminal region of each receptor subtype. Chimeric α_{1A}-AR displayed marked basal and agonist-induced phosphorylation (in contrast to the wild-type α_{1A}-AR), whereas the opposite was observed in chimeric α_{1B}-AR (34). The rapid decline of the α_{1B}/α_{1A}-CT-induced DAG signal upon overexpression of WT PKCδ supports the idea that the C ter-

minus represents a transferable element that confers PKCδ sensitivity of α_{1A}-AR to α_{1B}-AR. In contrast, overexpression of WT PKCδ failed to modulate α_{1B}-AR-induced DAG signals (Fig. 6). However, the inhibition of α_{1B}-AR desensitization with BAPTA and Gö6976 favors the idea that cPKCs rather than nPKCs contribute to receptor phosphorylation and desensitization. The most striking result of the present study is the fact that receptor desensitization did not abolish, but instead fine-tuned the effector response downstream of $G\alpha_q$. We measured K^+ currents through KCNQ1/KCNE1 channels (I_{Ks}) as a sensitive effector system downstream of $G\alpha_q$ activation and related receptor species-dependent desensitization to different time courses of I_{Ks} modulation. In our study, the time course of I_{Ks} modulation upon activation of α_{1B}-AR (Fig. 3*A*) is characterized by an inhibitory component related to PIP_2-induced current inhibition and subsequent I_{Ks} facilitation that is due to phosphorylation of the channel protein. Although the rapid desensitization of the α_{1B}-AR limits PIP_2 depletion and diminishes I_{Ks} inhibition, the activation of PKC facilitates I_{Ks} amplitude at the same time, resulting in net reduction of the inhibitory component to about 15% as compared with the initial current amplitude (Fig. 3*C*). Such a biphasic time course of I_{Ks} regulation upon activation of G_qPCRs has been described in previous studies (19, 20, 27), but to present a novel finding, we provide detailed insights into the contribution of different PKC isoforms to channel regulation. By using pharmacological tools (Fig. 6), we were able to dissect the contribution of different PKC isoforms to α_{1B} receptor desensitization (mediated by Ca^{2+}-dependent PKC isoforms) and I_{Ks} facilitation (PKCδ). Pharmacological inhibition of all PKC isoforms eliminates α_{1B}-AR desensitization and I_{Ks} facilitation, thus augmenting the inhibitory current component related to PIP_2 depletion.

In contrast to the α_{1B}-induced biphasic time course of I_{Ks} modulation, stimulation of muscarinic receptors induced sustained PIP_2 depletion (Fig. 2), resulting in net inhibition of I_{Ks} of about 30% (Fig. 3), but no PKC-induced I_{Ks} facilitation. As indicated by Fig. 4, M_1-R-induced PIP_2 depletion was sustained during agonist exposure, in line with the fact that M_1 receptors reveal no desensitization in the presence of acetylcholine. According to a kinetic model by Matavel and Lopes (13) and confirmed by our own results presented above, the time course of I_{Ks} modulation is the result of an interplay of PIP_2 depletion and PKC activation. In a previous study, PKC activation upon stimulation of M_1-R has been demonstrated by using the FRET reporter system PKC-CKAR (C kinase activity reporter), but because PKC activation is saturated by small amounts of DAG (5), this biosensor is not suitable to investigate different receptor species-dependent efficiencies of PKC activation. Notably, neither inhibition of Ca^{2+}-dependent/Ca^{2+}-independent isoforms nor overexpression of PKCδ induced M_1 receptor desensitization during agonist exposure; rather, they excluded the significant contribution of PKC to M_1-R-induced I_{Ks} modulation. It is conceivable that pronounced PIP_2 depletion during M_1-R stimulation overrides a potential PKC-induced I_{Ks} facilitation. However, our data suggest that pronounced PIP_2 depletion *per se* does not inhibit PKCδ activation. Removal of α_{1B}-AR desensitization by PKC inhibitors (staurosporine and Gö6976) increases the inhibitory current component to a similar extent (~25%) as observed during M_1-R stimulation (~30%), indicating similar efficiencies of α_{1B}-ARs and M_1-Rs in PIP_2 depletion. However, I_{Ks} facilitation is still observed during inhibition of cPKCs with Gö6976 (Fig. 9*C*), indicating that PKCδ activation is not abrogated upon pronounced PIP_2 depletion. In the absence of PKC inhibitors, rapid desensitization of α_{1B}-ARs reduces the inhibitory effect of PIP_2 depletion and shifts I_{Ks} activity toward I_{Ks} facilitation by simultaneous activation of nPKCs. In contrast, stimulation of M_1-R induced sustained PIP_2 depletion, but obviously no PKC activation, thus shifting the fine-tuning of I_{Ks} activity toward current inhibition.

To summarize, receptor-specific desensitization is a mechanism of effector modulation by restricting the spatiotemporal activation of downstream G_q signaling components. Receptor-dependent differences in desensitization account for different I_{Ks} modulation by α_{1B}-AR and M_1-R by controlling the duration of PIP_2 depletion and the recruitment of different PKC isoforms.

Experimental Procedures

Molecular Biology and Cell Culture—To generate fusion proteins of α-ARs, the cDNA fragments indicated below were generated by PCR and inserted into linearized pcDNA3 (Invitrogen) using the In-Fusion cloning method (Clontech) following the manufacturer's instructions. To generate YFP-labeled versions of the human α_{1B}-AR (NM_000679), yellow fluorescent protein (YFP) was amplified by PCR and either attached to the C terminus of the receptor or inserted between amino acids (aa) 253 and 254. The latter results in a receptor that carries YFP in its third intracellular loop, which is not expected to interfere with phosphorylation of the C terminus. The constructs were termed α_{1B}-AR-YFP or α_{1B}-AR-YFP-IL3, respectively. To generate a chimeric α_{1A}/α_{1B}-AR, a cDNA fragment encoding for aa 1–351 of human α_{1B}-AR was directly fused to a fragment encoding for the C terminus (aa 330–466) of human α_{1A}-AR (NM_000680). This construct was termed α_{1B}/α_{1A}-CT chimera. All constructs were verified by DNA sequencing. The aa positions refer to entries P35348 (α_{1A}-AR) and P35368 (α_{1B}-AR) of the UniProt database.

All experiments were performed using either CHO cells stably expressing the subunits KCNQ1/KCNE1 underlying I_{Ks} (45) or native HEK 293 cells. CHO cells were grown in Iscove's modified Dulbecco's medium containing fetal bovine serum (10%), HT supplement, non-essential amino acids, and 400 μg/ml G-418. HEK 293 cells were grown in DMEM medium, supplemented with glutamine (1%) and fetal calf serum (10%). Both cell lines were cultured with penicillin/streptomycin using standard cell culture conditions. All cell culture media and supplements were purchased from Gibco. Both cell lines were transiently transfected with cDNAs encoding for G_qPCRs and the following FRET biosensors (amount in μg per 3-cm culture dish). To monitor the G_q protein cycle, we used α_1-ARs (0.5) or M_1-R (0.5), $G\alpha_q$-YFP (1.0), $G\beta_1$-Cerulean (0.5), $G\gamma_2$ (0.2), and GPCR kinase 2 (GRK2) (0.5) (17). To monitor receptor-arrestin interactions, we used α_{1B}-AR-YFP or M_1-R-YFP (0.6), Turquoise-arrestin3 (0.6), and GRK2 (0.8) (24). To monitor the breakdown of PIP_2 as a measure for PLC activation, we used receptor species as indicated (0.5) and a PIP_2 biosensor (0.5)

that is based on CFP- and YFP-labeled PH domains of PLCδ1 (22). To monitor the production of the second messenger DAG, we used receptor species as indicated (0.5) and the biosensor DAGR (0.5), which reports conformational changes of a CFP/YFP-labeled DAG-binding domain of protein kinase C (PKCβ2) (18). DAGR was kindly provided by Dr. Alexandra Newton (Addgene plasmid number 14865). For some experiments, cells were cotransfected with 0.5 μg of a plasmid encoding for WT PKCδ or PKCδ DN (29), kindly provided by Dr. Bernard Weinstein via Addgene (WT, plasmid number 16386, and DN, plasmid number 16389). Functionality of WT PKCδ and PKCδ DN was confirmed in experiments on KCNQ1/KCNE1-expressing CHO cells measuring I_{Ks} modulation during α_{1B} receptor stimulation (see supplemental Fig. S4). Both cell lines were transfected using either polyethyleneimine as described in Ref. 22 or Lipofectamine (Invitrogen) according to the manufacturer's instructions. Prior to experiments, cells were seeded on sterile, poly-L-lysine-coated glass coverslips and analyzed 24 h (cells expressing DAGR) or 48 h after transfections.

Fluorescence Microscopy and Imaging—All experiments were performed using single cells at ambient temperature. Fluorescence was recorded using an inverted microscope (Zeiss Axiovert 200, Carl Zeiss AG, Göttingen, Germany) equipped with a Zeiss oil immersion objective (100×/1.4), a Polychrome V illumination source, and a photodiode-based dual emission photometry system suitable for CFP/YFP FRET (TILL Photonics/FEI GmbH, Munich, Germany). For FRET measurements, single cells were excited at 435-nm wavelength with light pulses of variable duration (10–50 ms) at a frequency of 5 Hz to minimize photobleaching. Corresponding emitted fluorescence from CFP (F_{480} or F_{CFP}) or from YFP (F_{535} or F_{YFP}) was acquired simultaneously, and FRET was defined as ratio F_{YFP}/F_{CFP}. Fluorescent signals were recorded and digitized using a commercial hardware/software package (EPC10 amplifier with an integrated D/A board and Patchmaster software, HEKA, HEKA Elektronik, Lambrecht/Pfalz, Germany). Details on optical filters and beam splitters of the setup are given in Ref. 22. The individual FRET traces for obtaining concentration-response curves were normalized to the maximal response of the G protein biosensor at saturating agonist concentrations (FRET/$FRET_{10\ \mu M}$), denoted as FRET/$FRET_{max}$). All other traces were normalized to the initial ratio value before agonist application (FRET/$FRET_0$). For receptor internalization experiments, YFP was excited at 500 nm, and fluorescence images were acquired with a Zeiss AxioCam MRm epifluorescence camera and corresponding AxioVision software. After application of phenylephrine, consecutive pictures were taken after the incubation times as indicated.

Current Measurement—Membrane currents were measured using whole-cell patch clamp technique. Pipettes were fabricated from borosilicate glass and filled with the solution listed below (direct current resistance, 4–6 megaohms). Currents were measured by means of a patch clamp amplifier (LM/EPC 7, List Electronics, Darmstadt, Germany). Signals were filtered (corner frequency, 1 KHz), digitally sampled at 1 KHz, and stored on a computer equipped with a hardware/software package (ISO2, MFK, Frankfurt/Main, Germany) for voltage control and data acquisition. Experiments were performed at ambient temperature (23–26 °C). For combined patch clamp and FRET measurements, standard patch clamp equipment was attached to the optical setup. Application of different solutions was performed by means of a custom-made solenoid-operated flow system. Whole-cell I_{Ks} was routinely measured during depolarizing pulses (to + 60 mV, duration 5 s, applied every 20 s) from a holding potential of −80 mV (see also supplemental Fig. S5).

Solution and Chemicals—For whole-cell measurements of membrane currents an extracellular solution of the following composition was used (in mM): 137 NaCl; 5.4 KCl; 0.5 $CaCl_2$; 1.0 $MgCl_2$; 10.0 Hepes/NaOH, pH 7.4. The standard pipette solution contained (in mM): 100 potassium aspartate; 40 KCl; 5.0 NaCl, 2.0 $MgCl_2$; 5.0 Na_2ATP; 2.0 EGTA; 0.025 GTP; 20.0 HEPES/KOH, pH 7. Where indicated, EGTA was replaced by 5 mM BAPTA. Standard chemicals were from Merck (Darmstadt, Germany). BAPTA, EGTA, HEPES, Na_2ATP, phenylephrine, sodium salt hydrate (GTP), and ACh were from Sigma-Aldrich (Taufkirchen, Germany). Staurosporine and Gö6976 were purchased from Tocris Bioscience (Bristol, UK).

Statistical Analysis—All data are presented as individual observations or summarized data (mean ± S.E. of *n* cells). Student's *t* test was used to compare the means between two groups. *p* values less than 0.05 were considered statistically significant.

Author Contributions—M.-C. K., L. P., and A. R. participated in research design. M.-C. K., D. V., and C. M. conducted experiments and performed data analysis. M.-C. K., L. P., and A. R. wrote the manuscript or contributed to the manuscript.

Acknowledgments—We thank Anke Galhoff for expert technical assistance. We are thankful to Dr. Moritz Bünemann for providing G_q and arrestin FRET biosensors.

References

1. Berridge, M. J. (1987) Inositol trisphosphate and diacylglycerol: two interacting second messengers. *Annu. Rev. Biochem.* **56,** 159–193
2. Hubbard, K. B., and Hepler, J. R. (2006) Cell signalling diversity of the $G_q\alpha$ family of heterotrimeric G proteins. *Cell. Signal.* **18,** 135–150
3. Cho, H., Kim, Y. A., Yoon, J.-Y., Lee, D., Kim, J. H., Lee, S. H., and Ho, W.-K. (2005) Low mobility of phosphatidylinositol 4,5-bisphosphate underlies receptor specificity of G_q-mediated ion channel regulation in atrial myocytes. *Proc. Natl. Acad. Sci. U.S.A.* **102,** 15241–15246
4. Dickson, E. J., Falkenburger, B. H., and Hille, B. (2013) Quantitative properties and receptor reserve of the IP_3 and calcium branch of G_q-coupled receptor signaling. *J. Gen. Physiol.* **141,** 521–535
5. Falkenburger, B. H., Dickson, E. J., and Hille, B. (2013) Quantitative properties and receptor reserve of the DAG and PKC branch of G_q-coupled receptor signaling. *J. Gen. Physiol.* **141,** 537–555
6. Shirai, Y., and Saito, N. (2002) Activation mechanisms of protein kinase C: maturation, catalytic activation, and targeting. *J. Biochem.* **132,** 663–668
7. Mochly-Rosen, D., Das, K., and Grimes, K. V. (2012) Protein kinase C, an elusive therapeutic target? *Nat. Rev. Drug Discov.* **11,** 937–957
8. Hoque, M., Rentero, C., Cairns, R., Tebar, F., Enrich, C., and Grewal, T. (2014) Annexins: scaffolds modulating PKC localization and signaling. *Cell. Signal.* **26,** 1213–1225
9. Steinberg, S. F. (2008) Structural basis of protein kinase C isoform function. *Physiol. Rev.* **88,** 1341–1378
10. Gallegos, L. L., Kunkel, M. T., and Newton, A. C. (2006) Targeting protein kinase C activity reporter to discrete intracellular regions reveals spatio-

temporal differences in agonist-dependent signaling. *J. Biol. Chem.* **281,** 30947–30956
11. Hui, X., Reither, G., Kaestner, L., and Lipp, P. (2014) Targeted activation of conventional and novel protein kinases C through differential translocation patterns. *Mol. Cell. Biol.* **34,** 2370–2381
12. Gamper, N., Reznikov, V., Yamada, Y., Yang, J., and Shapiro, M. S. (2004) Phosphatidylinositol 4,5-bisphosphate signals underlie receptor-specific $G_{q/11}$-mediated modulation of N-type Ca^{2+} channels. *J. Neurosci.* **24,** 10980–10992
13. Matavel, A., and Lopes, C. M. (2009) PKC activation and PIP_2 depletion underlie biphasic regulation of I_{Ks} by G_q-coupled receptors. *J. Mol. Cell. Cardiol.* **46,** 704–712
14. Masuho, I., Ostrovskaya, O., Kramer, G. M., Jones, C. D., Xie, K., and Martemyanov, K. A. (2015) Distinct profiles of functional discrimination among G proteins determine the actions of G protein-coupled receptors. *Sci. Signal.* **8,** ra123
15. Bodmann, E.-L., Wolters, V., and Bünemann, M. (2015) Dynamics of G protein effector interactions and their impact on timing and sensitivity of G protein-mediated signal transduction. *Eur. J. Cell Biol.* **94,** 415–419
16. Chen, X., Egly, C., Riley, A. M., Li, W., Tewson, P., Hughes, T. E., Quinn, A. M., and Obukhov, A. G. (2014) PKC-dependent phosphorylation of the H1 histamine receptor modulates TRPC6 activity. *Cells* **3,** 247–257
17. Falkenburger, B. H., Jensen, J. B., and Hille, B. (2010) Kinetics of M_1 muscarinic receptor and G protein signaling to phospholipase C in living cells. *J. Gen. Physiol.* **135,** 81–97
18. Violin, J. D., Zhang, J., Tsien, R. Y., and Newton, A. C. (2003) A genetically encoded fluorescent reporter reveals oscillatory phosphorylation by protein kinase C. *J. Cell Biol.* **161,** 899–909
19. Matavel, A., Medei, E., and Lopes, C. (2010) PKA and PKC partially rescue long QT type 1 phenotype by restoring channel-PIP_2 interactions. *Channels (Austin)* **4,** 3–11
20. O-Uchi, J., Rice J. J., Ruwald, M. H., Parks, X. X., Ronzier, E., Moss, A. J., Zareba, W., and Lopes, C. M. (2015) Impaired I_{Ks} channel activation by Ca^{2+}-dependent PKC shows correlation with emotion/arousal-triggered events in LQT1. *J. Mol. Cell. Cardiol.* **79,** 203–211
21. van der Wal, J., Habets, R., Várnai, P., Balla, T., and Jalink, K. (2001) Monitoring agonist-induced phospholipase C activation in live cells by fluorescence resonance energy transfer. *J. Biol. Chem.* **276,** 15337–15344
22. Hertel, F., Switalski, A., Mintert-Jancke, E., Karavassilidou, K., Bender, K., Pott, L., and Kienitz, M. C. (2011) A genetically encoded tool kit for manipulating and monitoring membrane phosphatidylinositol 4,5-bisphosphate in intact cells. *PLoS One* **6,** e20855
23. Luttrell, L. M., and Gesty-Palmer, D. (2010) Beyond desensitization: physiological relevance of arrestin-dependent signaling. *Pharmacol. Rev.* **62,** 305–330
24. Krasel, C., Bünemann, M., Lorenz, K., and Lohse, M. J. (2005) β-Arrestin binding to the β_2-adrenergic receptor requires both receptor phosphorylation and receptor activation. *J. Biol. Chem.* **280,** 9528–9535
25. Castillo-Badillo, J. A., Sánchez-Reyes, O. B., Alfonzo-Méndez, M. A., Romero-Ávila, M. T., Reyes-Cruz, G., and García-Sáinz, J. A. (2015) α_{1B}-adrenergic receptors differentially associate with Rab proteins during homologous and heterologous desensitization. *PLoS One* **10,** e0121165
26. García-Sáinz, J. A., Romero-Ávila, M. T., and Alcántara-Hernández, R. (2011) Mechanisms involved in α_{1B}-adrenoceptor desensitization. *IUBMB Life* **63,** 811–815
27. O-Uchi, J., Sorenson, J., Jhun, B. S., Mishra, J., Hurst, S., Williams, K., Sheu, S.-S., and Lopes, C. M. B. (2015) Isoform-specific dynamic translocation of PKC by α_{1B}-adrenoceptor stimulation in live cells. *Biochem. Biophys. Res. Commun.* **465,** 464–470
28. Martiny-Baron, G., Kazanietz, M. G., Mischak, H., Blumberg, P. M., Kochs, G., Hug, H., Marmé, D., and Schächtele, C. (1993) Selective inhibition of protein kinase C isozymes by the indolocarbazole Gö 6976. *J. Biol. Chem.* **268,** 9194–9197
29. Soh, J.-W., and Weinstein, I. B. (2003) Roles of specific isoforms of protein kinase C in the transcriptional control of cyclin D1 and related genes. *J. Biol. Chem.* **278,** 34709–34716
30. Yeatman, H. R., Lane, J. R., Choy, K. H. C., Lambert, N. A., Sexton, P. M., Christopoulos, A., and Canals, M. (2014) Allosteric modulation of M_1 muscarinic acetylcholine receptor internalization and subcellular trafficking. *J. Biol. Chem.* **289,** 15856–15866
31. van Koppen, C. J., and Kaiser, B. (2003) Regulation of muscarinic acetylcholine receptor signaling. *Pharmacol. Ther.* **98,** 197–220
32. Willets, J. M., Nelson, C. P., Nahorski, S. R., and Challiss, R. A. J. (2007) The regulation of M_1 muscarinic acetylcholine receptor desensitization by synaptic activity in cultured hippocampal neurons. *J. Neurochem.* **103,** 2268–2280
33. Lattion, A. L., Diviani, D., and Cotecchia, S. (1994) Truncation of the receptor carboxyl terminus impairs agonist-dependent phosphorylation and desensitization of the α_{1B}-adrenergic receptor. *J. Biol. Chem.* **269,** 22887–22893
34. Vázquez-Prado, J., Medina, L. C., Romero-Avila, M. T., González-Espinosa, C., and García-Sáinz, J. A. (2000) Norepinephrine- and phorbol ester-induced phosphorylation of α_{1A}-adrenergic receptors: functional aspects. *J. Biol. Chem.* **275,** 6553–6559
35. Diviani, D., Lattion, A. L., and Cotecchia, S. (1997) Characterization of the phosphorylation sites involved in G protein-coupled receptor kinase- and protein kinase C-mediated desensitization of the α_{1B}-adrenergic receptor. *J. Biol. Chem.* **272,** 28712–28719
36. Stanasila, L., Abuin, L., Dey, J., and Cotecchia, S. (2008) Different internalization properties of the α_{1A}- and α_{1B}-adrenergic receptor subtypes: the potential role of receptor interaction with β-arrestins and AP50. *Mol. Pharmacol.* **74,** 562–573
37. Zhong, H., and Minneman, K. P. (1999) α1-Adrenoceptor subtypes. *Eur. J. Pharmacol.* **375,** 261–276
38. Felder, C. C. (1995) Muscarinic acetylcholine receptors: signal transduction through multiple effectors. *FASEB J.* **9,** 619–625
39. Violin, J. D., Dewire, S. M., Barnes, W. G., and Lefkowitz, R. J. (2006) G protein-coupled receptor kinase and β-arrestin-mediated desensitization of the angiotensin II type 1A receptor elucidated by diacylglycerol dynamics. *J. Biol. Chem.* **281,** 36411–36419
40. García-Sáinz, J. A., Vázquez-Prado, J., and del Carmen Medina, L. (2000) α1-Adrenoceptors: function and phosphorylation. *Eur. J. Pharmacol.* **389,** 1–12
41. Diviani, D., Lattion, A. L., Larbi, N., Kunapuli, P., Pronin, A., Benovic, J. L., and Cotecchia, S. (1996) Effect of different G protein-coupled receptor kinases on phosphorylation and desensitization of the α_{1B}-adrenergic receptor. *J. Biol. Chem.* **271,** 5049–5058
42. Iacovelli, L., Franchetti, R., Grisolia, D., and De Blasi, A. (1999) Selective regulation of G protein-coupled receptor-mediated signaling by G protein-coupled receptor kinase 2 in FRTL-5 cells: analysis of thyrotropin, α_{1B}-adrenergic, and A_1 adenosine receptor-mediated responses. *Mol. Pharmacol.* **56,** 316–324
43. Toews, M. L., Prinster, S. C., and Schulte, N. A. (2003) Regulation of α_{1B}-adrenergic receptor localization, trafficking, function, and stability. *Life Sci.* **74,** 379–389
44. Perez-Aso, M., Segura, V., Montó, F., Barettino, D., Noguera, M. A., Milligan, G., and D'Ocon, P. (2013) The three α_1-adrenoceptor subtypes show different spatio-temporal mechanisms of internalization and ERK1/2 phosphorylation. *Biochim. Biophys. Acta* **1833,** 2322–2333
45. Kienitz, M.-C., and Vladimirova, D. (2015) Synergistic modulation of KCNQ1/KCNE1 K^+ channels (I_{Ks}) by phosphatidylinositol 4,5-bisphosphate (PIP_2) and $[ATP]_i$. *Cell. Signal.* **27,** 1457–1468